UCRL-9823

UNIVERSITY OF CALIFORNIA

Ernest O. Lawrence Radiation Laboratory

BERKELEY, CALIFORNIA

Proceedings of 1st Int. Biophys. Congress
Stockholm July 31-Aug. 6, 1961
(Published by Pergamon Press)

UCRL-9823
Limited Distribution

UNIVERSITY OF CALIFORNA
Lawrence Radiation Laboratory
Berkeley, California

Contract No. W-7405-eng-48

ELECTRON PARAMAGNETIC RESONANCE IN BIOLOGY

G. M. Androes and Melvin Calvin

August 15, 1961

UCRL-9823

ELECTRON PARAMAGNETIC RESONANCE IN BIOLOGY*

G. M. Androes and Melvin Calvin

Department of Chemistry and Lawrence Radiation Laboratory**
University of California, Berkeley 4, California

August 15, 1961

Abstract

A review of the theories of electron paramagnetic resonance in biology is presented, including a discussion of the nature of the physical observation, followed by examples of materials of biological interest. In discussing these examples, information is presented in terms of the nature of the starting material under observation rather than the nature of the magnetic entities observed. The examples proceed from the simpler molecules of biological interest (metabolites, vitamins, cofactors) into the more complex materials (polymers, proteins, nucleic acids) toward cellular organelles (mitochondria, chloroplasts) and, finally, to whole cells, organisms and organs.

The observation of photoinduced unpaired electrons in photosynthetic material is described and the various parameters controlling it are discussed. The basic observation is interpreted in terms of a primary photophysical act of quantum conversion.

---

* Presented at First International Biophysics Congress, Stockholm, Sweden, July 31-Aug. 5, 1961.

** The preparation of this paper was sponsored by the U.S. Atomic Energy Commission.

ELECTRON PARAMAGNETIC RESONANCE IN BIOLOGY*

G. M. Androes and Melvin Calvin**

Department of Chemistry and Lawrence Radiation Laboratory***
University of California, Berkeley 4, California

---

* Presented at First International Biophysics Congress, Stockholm, Sweden, July 31-August 5, 1961.

** Research Professor of Chemistry in the Miller Institute for Basic Research in Science, University of California, Berkeley.

*** The preparation of this paper was sponsored by the U.S. Atomic Energy Commission.

I. INTRODUCTION.

The material of which living organisms are made is largely organic. Even the inorganic constituents, aside from the sodium chloride, are most often found very closely associated with, if not a component part of, organic substances in living organisms. The structure and change of structure of such materials, that is, organic substances in general, is determined by the electronic configuration of the atoms of which they are made, and by changes in these electronic configurations. Therefore, any method of observation which permits us to look closely into the nature of the electronic configurations and the changes of these electronic configurations is likely to become a major tool in biological studies.

One such method of observation which has recently (that is, in the last decade or so) risen to prominence, particularly in the study of the electronic structure of inorganic materials, is now becoming of importance in the examination both of the statics and dynamics of organic and biological materials. This method depends upon the fact that a spinning electron is magnetic as are, in fact, a good many nuclei as well. Therefore, such an electron, when placed in an external magnetic field,

will interact with that field in a characteristic way which can be determined by suitable configuration of the magnet and electromagnetic radiation, which we will discuss later.

Now not all the electrons present in chemical substances can be studied by such magnetic resonance methods. Only those substances which contain in them magnetic entities which can respond to an external magnetic field in an observable way are likely to yield information. Certain nuclei of considerable interest to us do have such properties, and we will mention them later.

Most of the electrons in organic materials, however, although they individually do have a spin and a magnetic moment, exist in the organic material in pairs in which the magnetic moments are oppositely directed and are closely coupled so that the individual electrons cannot interact in an as yet observable fashion with an external magnetic field. We are therefore limited in our biological exploitation of this method to such materials that contain electrons not so paired. Since many important chemical transformations which occur in biological materials involve at some stage of their occurence the uncoupling of these paired electrons in some way or another, it seems likely that this method of observation will find a broad application in the study of biological structures and their changes.

Materials which contain electrons in any of the following conditions might be susceptible to study by electron paramagentic resonance methods, and many of them have already been observed in biological materials:

(a) Free electrons: Such electrons as are found as conduction electrons in a metal are indeed free, and under certain special conditions their spin lifetimes are sufficiently long so that they may be observed by these methods.

(b) Not-quite-free electrons: Such electrons as are found in the narrow conduction bands in semiconductors are also susceptible to observation. These electrons are produced by being raised from bound, or coupled, states into their conduction, or free, states, usually by temperature or light.

(c) Trapped "free" electrons: These are electrons which are not paired but which are physically trapped in a solid lattice (either ionic, atomic or molecular) and are definitely readily observable by this method.

(d) Unpaired electrons from paired electrons: These unpaired electrons, created by the fission of a paired electron bond which generally involves the separation of atoms as well, are also clearly observable by these methods. Such (ordered) molecules may appear as chemical reaction intermediates or as broken bonds created by high energy radiation.

(e) Unpaired electrons in even molecules: These are unpaired electrons from molecules containing an even number of electrons in which two or more have been uncoupled to form what is called a state of higher multiplicity. (When only one electron pair is uncoupled to give two electrons with parallel spin moments, it is called a triplet state.)

(f) Unpaired electrons from transition metal ions: These electrons in the transition metal ions such as iron, cobalt, nickel and copper are generally observable by the method of electron spin resonance. It is clear that these unpaired electrons, existing as they do in the d-orbitals of transition elements, are quite common in biological systems. Unfortunately, they are not always observed, at least under the conditions which are currently known to us. However, much important information is beginning to appear in studies of this sort.

The course of our examination will be divided into two distinct parts, the first of which is the nature of the physical observation itself. We will describe all of the parameters associated with the observation of unpaired electrons, that can be determined. Some of these are already in common use, and others have not yet achieved usefulness in the biological sphere and we will try to indicate those.

Finally, a collection of examples of the examination of materials of biological interest will be provided. Such a wide literature already exists that it will be beyond our capacity to catalog them all. However, we will try to provide examples of all the types of observations that have been made and indicate those which are still possible but which have not yet been achieved.

The pattern followed in the presentation of biological examples has been difficult to formulate, largely because the unifying principle here is a technique of observation rather than a biological principle. However, the general pattern has been the use of the physical tool as it became available directly on very complex biological material to demonstrate that there were indeed such magnetic entities as unpaired electrons present in biological materials under suitable conditions. The next step, however, of identifying and characterizing those entities has proved to be much more difficult and it has required a retrenchment toward the simpler systems in order to learn more of the nature of the observation itself.

We will, therefore, present the examples in terms of the nature of the starting material under observation rather than the nature of the magnetic entities observed, since we do not really know the latter in most cases. We will proceed from the simpler molecules of biological interest -- such as metabolites, vitamins, cofactors, etc. -- into the more complex materials -- such as polymers, proteins, nucleic acids -- toward cellular organelles -- mitochondria, chloroplasts and the like -- and, finally, to whole cells, organisms, and organs. This will be the exposition, in spite of the fact that historically observations have been made in somewhat the reverse order.

II. PHYSICS WITH EXAMPLES.

A. Zeeman Energy Levels.

If an atomic or molecular system with spin angular momentum of magnitude $\hbar\sqrt{S(S+1)}$ is placed in a magnetic field, H, the component of angular momentum along the direction of the field may assume only the values

$$S\hbar, (S-1)\hbar, \ldots\ldots\ldots\ldots\ldots, -S\hbar.$$

Each of these 2S + 1 orientations will have a different energy. The energy of these states, the Zeeman energy, may be written

$$\mathcal{H} = g\beta \vec{H}\cdot\vec{S} = g\beta H_z m_s$$

if H is in z direction and $m_s = S, S-1, \ldots\ldots\ldots\ldots, -S$. According to the basic quantum mechanical principle, transitions between these magnetic states can be induced by providing a quantum of energy $h\nu$, of the appropriate size.

Except under special circumstances, transitions may be induced only between adjacent levels: i.e. $\Delta m_s = \pm 1$, Thus, the condition for inducing the transitions (the resonance condition) is $h\nu = g\beta H_z$. In this expression $\beta = \frac{e\hbar}{2mc}$ is the Bohr magneton, and g represents the effective size of the magnetic moment being acted upon by the magnetic field. It is equivalent to the spectroscopic splitting factor,

$$g = 1 + \frac{J(J+1) + S(S+1) - L(L+1)}{2\,J(J+1)}$$

of the free atom. (1) When H is 3300 gauss and g = 2.00, ν is 9.5 Kmc/s. ($\lambda \sim 3.2$ cm.)

B. Resonant Energy Absorption.

When the resonance condition is satisfied, transitions from m_s to $m_s + 1$ and from $m_s + 1$ to m_s are induced with equal probability by the high frequency (microwave) magnetic field. This in itself leads to no energy absorption. A net energy absorption arises from two facts: 1) The spin system, in thermal

equilibrium, has a few more spins in the state m_s than in the state $m_s + 1$. The slightly greater number of spins in the states of lower energy means that slightly more transitions up than down will be induced by the microwave field. 2) There are alternate routes by which spins excited to the state $m_s + 1$ can be returned to m_s; the routes through which thermal equilibrium would be re-established should the microwave field be suddenly removed. These processes are called thermal relaxation processes.

The margin of operation for observation of the net energy absorbed is small. In Table I we have listed values for the Boltzman factor determining the population distribution, and the fractional spin unbalance for an S = 1/2 system at three different temperatures. It is seen that even at $4.2^{\circ}K$, of 100 spins there are only 5 more in the ground than in the excited state. The first person to observe these small energy absorptions was Zavoisky, in the USSR, in 1946. (2) He used solutions containing transition metal ions. In the United States, Cummerow and Halliday (3) made the first observations of this type in 1947. The field has been developing rapidly ever since.

We would now like to answer the following two questions: What are the measurable parameters associated with this resonance absorption? And, which of these, if any, might be useful in the solution of problems concerning biology?

C. Area under curve

The reaction of a system of free electrons to an applied magnetic field is depicted in Fig. 1a. In a resonance experiment (holding ν constant) each electron would absorb energy at exactly the same value of H_o (H_o and H_z are used interchangeably to identify the large applied field.) When unpaired electrons exist inside an actual sample the resonance condition is not satisfied at one unique applied field, but over a range of values. This is because a range of local magnetic fields is contributed by the sample itself.

	300°K	77°K	4.2°K
$\frac{g\beta H}{kT}$	1.48×10^{-3}	5.76×10^{-3}	1.05×10^{-1}
$\frac{n\uparrow - n\downarrow}{n\uparrow + n\downarrow}$	7.4×10^{-4}	2.9×10^{-3}	5.0×10^{-2}

$g = 2.00$; $\beta = 0.927 \times 10^{-20}$ erg/gauss; $H = 3300$ gauss

Table I.

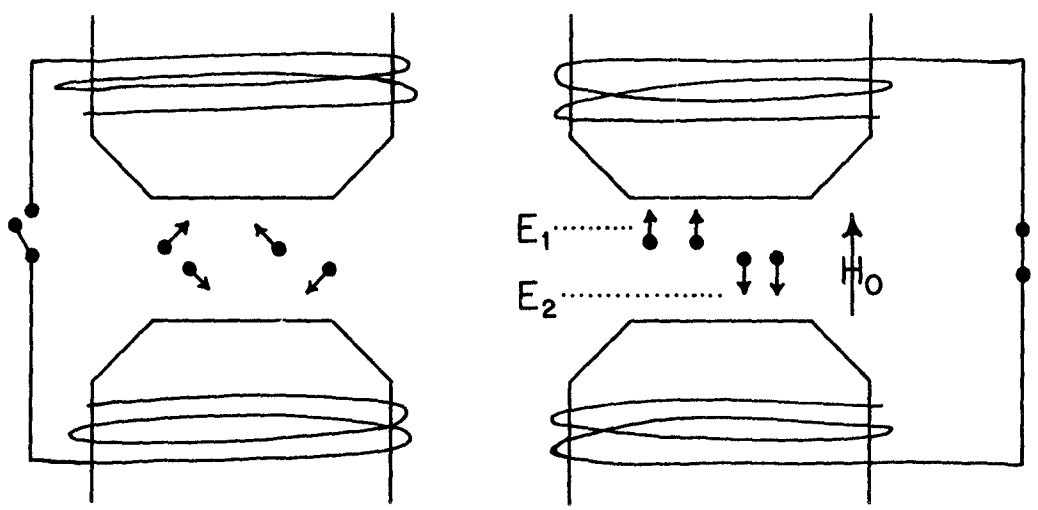

$$E_2 - E_1 = \mu_0 \cdot g_0 \cdot H_0 = \Delta E = h \cdot \nu = h \cdot c / \lambda$$

$$\lambda = \frac{h \cdot c}{\mu_0 \cdot g_0 \cdot H_0} \qquad \mu_0 = 0.927 \cdot 10^{-20} \qquad H_0 = 3{,}300 \qquad \lambda \sim 3{,}2 \text{ cm}$$

Fig. 1a. Diagramatic representation of the behavior of a population of free electrons in an external magnetic field.

These add vectorially to H_o to produce the effective resonance field at a particular electron (see below). In the simplest cases the net effect is to produce a resonance curve as shown in Fig. 1b.

As the resonance condition is traversed energy is absorbed from the microwave field, causing an electrical unbalance in the spectrometer. This unbalance is proportional to the amplitude of the absorption curve (Fig. 1b) for a particular value of H_o. Recording the unbalance of the spectrometer as a function H_o will thus yield the absorption curve.

The sensitivity of the spectrometer can be considerably enhanced by causing the resonance absorption to unbalance the spectrometer sinusoidally at a frequency ν_m. One then looks specifically at the spectrometer unbalance occuring at frequency ν_m, any other frequency variation in unbalance being ignored. This scheme is accomplished, usually, by modulating H_o at frequency ν_m as H_o is also being slowly swept through the resonance condition (Fig. 1b). The unbalance that is recorded using this scheme is not proportional to the height of the absorption curve at the mean value of H_o at a given point, but is proportional to the difference in height of the absorption curve between the extremes of the modulation envelope. The resultant sinusoidal unbalance is designated "signal" in Fig. 1b. This, then, is the signal leaving the detector (Fig. 2). Its magnitude is proportional to the first derivative of the absorption curve.

In Fig. 2 the lock-in amplifier analyzes the detected and amplified signal for only those components varying at frequency ν_m. The magnitude of these components is recorded, and yields the first derivative of the absorption curve. This is the curve commonly observed in published work.

The integrated area under the absorption curve (the second integral of the derivative curve) is proportional to the number of magnetic species absorbing microwave power. For a voltage sensitive microwave detector and Lorentzian line shape function

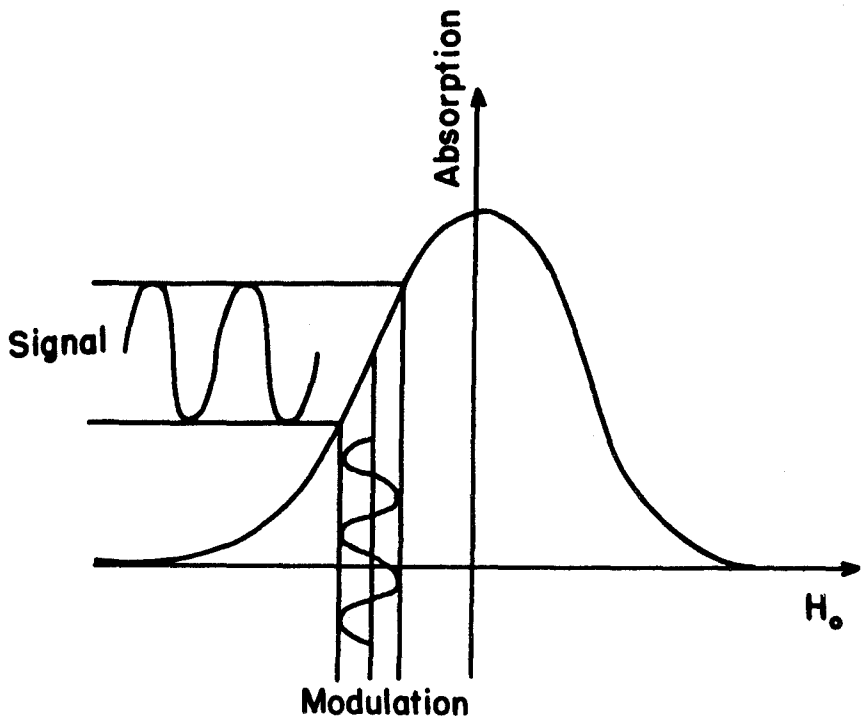

Fig. 1b. Field modulation applied to a resonance absorption, showing the origin of the derivative signal.

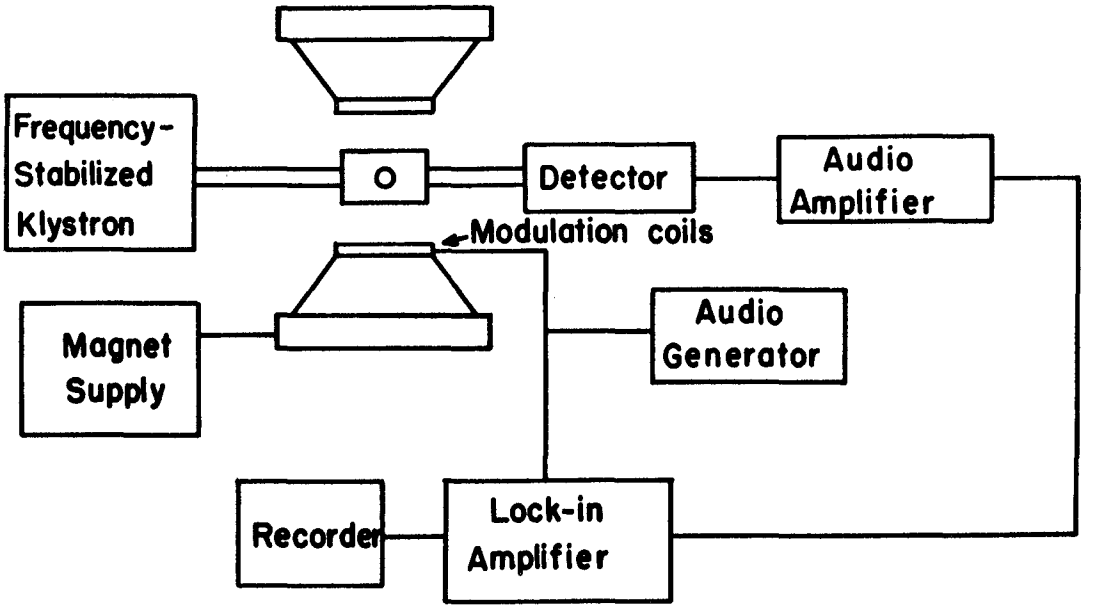

Fig. 2. Transmission spectrometer employing field modulation and phase sensitive detection. The microwave magnetic field, H_1, in the cavity is perpendicular to H_o, the applied magnetic field.

$$\text{Area} \propto \frac{H_1 Q_L \chi_o}{(1 + 1/4\gamma^2 H_1^2 T_1 T_2)^{1/2}}$$

where H_1 is the magnitude of the microwave magnetic field at the site of the sample, Q_L is the quality factor for the microwave cavity in place in the spectrometer, $\gamma = \omega_o/H_z$, T_1 is the spin lattice relaxation time (discussed below), and, for our purposes, T_2 defines the width of the absorption line.

$$\chi_o = \frac{N_o}{3KT} \quad g^2\beta^2 S(S + 1)$$

Here N_o is the number of spins per unit volume and T is the absolute temperature.

The constant of proportionality between area and N_o may be evaluated in terms of the gains, power, time constant, etc., of the spectrometer. It is easier and more accurate, however, to relate the area under the curve of an unknown to the area under the curve of a sample with a known number of spins.

In view of the form of the above factor, relating area to N_o, several facts should be observed. 1) The same microwave power level should be applied to both samples, and this power level should be such that both spin populations remain in thermal equilibrium with the lattice ($1/4\gamma^2 H_1^2 T_1 T_2 \ll 1$). 2) The two samples should effect the electrical properties of the microwave cavity in the same way (giving the same Q_L). 3) Most microwave spectrometers obtain the necessary sensitivity by modulating H_z and employing a phase sensitive detection system (Fig. 2). This modulation scheme broadens the absorption line. This must be taken into account, especially if a narrow line is compared with a wide one and the same modulation amplitude is used on both.

A double cavity, first used by Köhnlein and Müller (4), automatically takes points (1) and (2) into consideration. This cavity (Fig. 3) allows the simultaneous placement of both samples on equivalent nodal planes of the stationary microwave pattern of the cavity. Overlapping resonance lines are separated by using steel shims or Helmholz coils to provide an auxiliary field at one sample site.

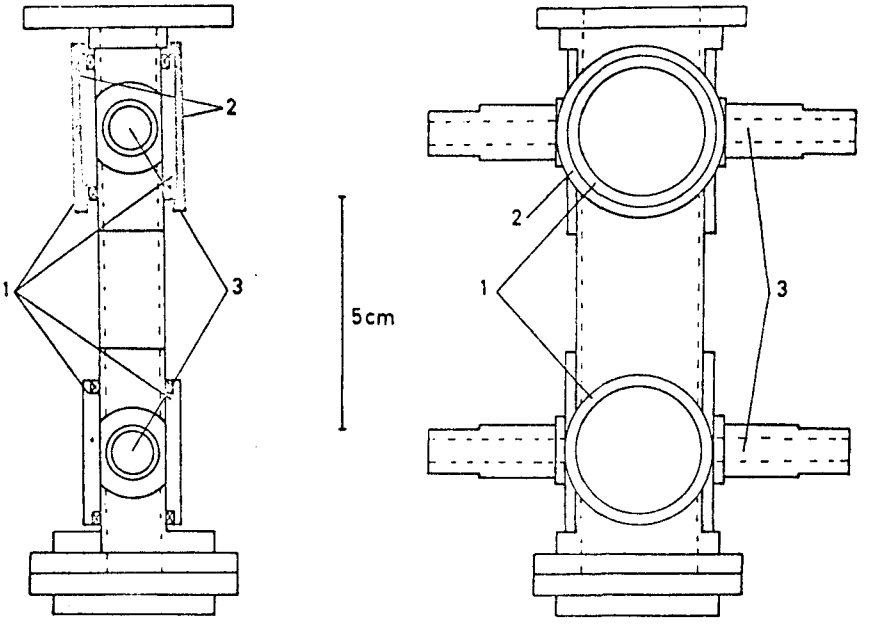

FIG. 1. Double cavity. (1) Modulation coils, (2) mild steel disks with shims, (3) sample holes.

Fig. 3. Double cavity. (1) Modulation coils, (2) mild steel disks with shims, (3) sample holes. (After 4).

We have used this type of cavity to advantage with samples whose dielectric loss properties vary greatly.

In some situations one wants to know the spin concentration only as a function of time or as a function of some other external variable. Then it is necessary only to follow some resonance parameter which is proportional to the area under the curve. Assuming the line shape and width do not change, the amplitude of the resonance is such a parameter.

D. Line Shapes.

A second measurable parameter is the structure of the resonant absorption. This is capable of providing quite detailed information about the environment of the observed magnetic species. Obviously, this is the sort of thing an experimenter using biological systems would delight in. Unfortunately, it is seldom observed in such samples.

The principal interaction which will produce structure in a resonance absorption is called the hyperfine or "contact" interaction. The name results from the fact that the electronic wave function must be in "contact" with the nucleus or the interaction is zero. The energy of this interaction may be written

$$\mathcal{H}_i = A\,\vec{I}\cdot\vec{S} = Am_I m_s$$

where A is a constant representing the strength of the interaction and I and S are the spin quantum numbers of the nuclear and electronic systems, respectively. The last form of the equation results from the fact that both spin moments are quantized along the same axis, (m_I = I, I-1,....., -(I-1), -I). This interaction is isotropic in space. Its effect is to split each electronic energy level into 2I + 1 levels. Hence, the resonance absorption is split into 2I + 1 equally spaced, equally intense lines.

Several cases may be distinguished.

(1) The electronic wave function is confined to one atom and is interacting with the nucleus of that atom. An example of this case appears in Fig. 4. The state of the 3d electrons contains some s character so that the Mn^{55} nucleus is seen. $I_{Mn}55 = 5/2$ so that a 6-line spectrum results.

(2) The electronic wave function is delocalized so that the interaction is equally distributed among several nucleii. In this case $I_t = \Sigma_i I_i$ and $2I_t + 1$ equally spaced lines result. However, now a statistical effect enters. A given value of $(m_I)_t$ may possibly be achieved with several different nuclear configurations. For example, the states with $(m_I)_t = \pm I_t$ can be achieved in only one way (all nuclear spins parallel), while the states with $(m_I)_t \sim 0$ can be made in several ways. The probability of these states (and thus the line intensities) follows the binomial coefficients. This type of behavior is shown for a series of halogenates semiquinones in Fig. 5.

(3) The electron is coupled primarily to one nucleus, but is delocalized enough to interact with neighboring nucleii -- a combination of (1) and (2). An example is shown in Fig. 6 for copper etioporphyrin-II. The example is not as ideal as one might like, but apparently the Cu^{++} electrons are coupled primarily to Cu^{63} ($I = 3/2$), and equally coupled to the four neighboring N^{14}. $I_N14 = 1$, so $I_t = 4$, and one expects 9 lines on each of the 4 lines resulting from the Cu^{63} coupling. Second order effects cause the Cu^{63} lines to vary in intensity. On the most intense line, 7 of the 9 lines expected are visible.

There are three nuclei of wide biological occurrence that have no nuclear moments and will thus not produce this type of structure. These are listed in Table II with several other nuclei from which splitting might be expected.

As mentioned above, resonance lines with well resolved structures are seldom seen in samples of biological materials. We shall next inquire as to why structures are sometimes unresolved, and what other parameters characteristic of such lines can be measured.

Fig. 4. The epr spectrum of Mn^{++} (at 200 molar ppm) in MgO.

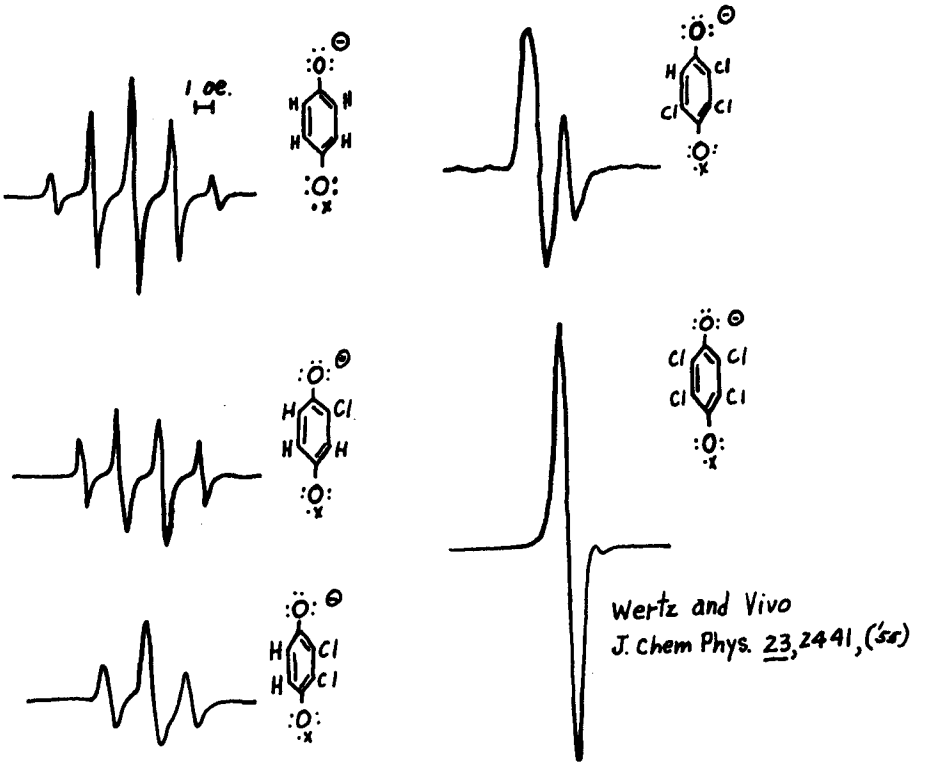

Fig. 5. The epr spectra of a series of chlorine-substituted semiquinones. (After 5).

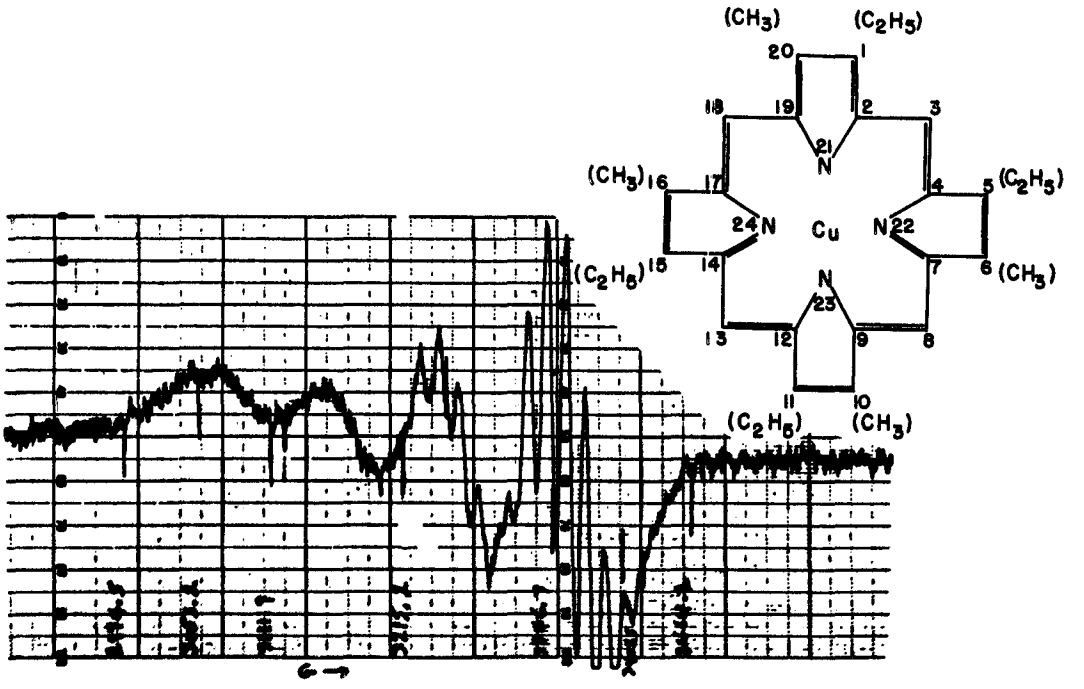

Fig. 6. The epr spectrum of CuEtio II in benzene. Inset, CuEtio II. (After 6).

STRUCTURE PRODUCING NUCLEII		
Isotope	Spin	% Abundance
H^{1}	1/2	99.9
N^{14}	1	99.6
P^{31}	1/2	100
Cl^{35}	3/2	75.4
Mn^{55}	5/2	100
Cu^{63}	3/2	69.1

NUCLEII WITHOUT MAGNETIC MOMENTS		
Isotope	Spin	% Abundance
C^{12}	0	98.9
O^{16}	0	99.8
S^{32}	0	95.1

Table II.

There are several mechanisms which might operate singly or in combinations to obliterate structures. In extreme cases, the entire line might become unobservable. Dipole-Dipole Broadening. This effect could be electron-electron (between neighboring molecules) or electron-nuclear (with nucleii on the same molecule). It results from the fact that the electrons and nucleii involved have magnetic moments associated with them. The field of a magnetic moment is anisotropic in space and can be averaged out by the tumbling action of a molecule in solution. In amorphous or multicrystalline solids a broadening results. The order of magnitude of the effect is approximated by the expression $\mu/r^3 \sim h$, where h is the local field produced at distance r from a spin with magnetic moment μ. For an electron $h \sim 80$ gauss when $r = 5$ Å. If this type of broadening is a problem, magnetic dilution of the sample (increasing the mean unpaired spin separation) is an obvious solution.

The line shape resulting from this type of broadening is approximately Gaussian. The resonance may be further classified as homogeneous; that is, every magnetic species being observed is equivalent. A spin found resonating in the low field wing of the resonance line may at a slightly later time be found resonating in the high field wing due to a change in its local environment.

Inhomogeneous Broadening. In distinction to the definition just given for a homogeneous line, a spin found resonating in the low field wing of an inhomogeneous line will always be found in that wing because its local environment will never change sufficiently (in the time of the experiment) to move it to any other section of the resonance. This type of broadening can be brought about, of course, by putting the sample in an inhomogeneous external magnetic field. In the more interesting cases the conditions inside the sample are such that the observed resonance is only the envelope of a large number of overlapping narrower lines. This is depicted on the left side of Fig. 12. The classic case of this kind is

F centers in ionic crystals. Here, there is a Gaussian distribution of types of magnetic sites. In the other extreme, an unresolved 5 or 7 line structure displays some of the characteristics of an inhomogeneous system.

Fig. 7 shows the idealized behavior of homogeneous and inhomogeneous systems as a function of microwave power. At very low levels, the increase in signal amplitude is approximately linear with power. As the microwave power is further increased the r.f. induced transitions begin to catch up with the thermal relaxation processes. Saturation begins to set in as the spin system departs from thermal equilibrium; the energy levels are becoming more and more equally populated. The saturation behavior of the homogeneous and inhomogeneous systems is distinctly different. In addition, the line width of the inhomogeneous system remains constant as the microwave power is increased, whereas the homogeneous system broadens. For example, the width of an homogeneous Lorentzian line (between points of maximum slope) increases as

$$T_2^{-1} (1 + 1/4 \gamma^2 H_1^2 T_1 T_2)^{1/2}.$$

Now, although each narrow line making up the envelope follows homogeneous behavior, the envelope as a whole does not; the broadening of any one component line is small compared to the width of the envelope; each individual component saturates in approximately the same way so the shape of the envelope does not change.

Exchange Narrowing. This may be thought of as resulting from the actual physical exchange of unpaired electrons among different magnetic environments in the sample. As the exchange becomes rapid, the electron will see an effective magnetic field which is some average of the local fields of the various sites. Because of the averaging effect resolved structure will collapse, with a single narrowed line resulting from sufficiently rapid exchange. The single line tends toward Lorentzian in shape.

Two cases will be mentioned. 1) The unpaired electron is exchanging with other

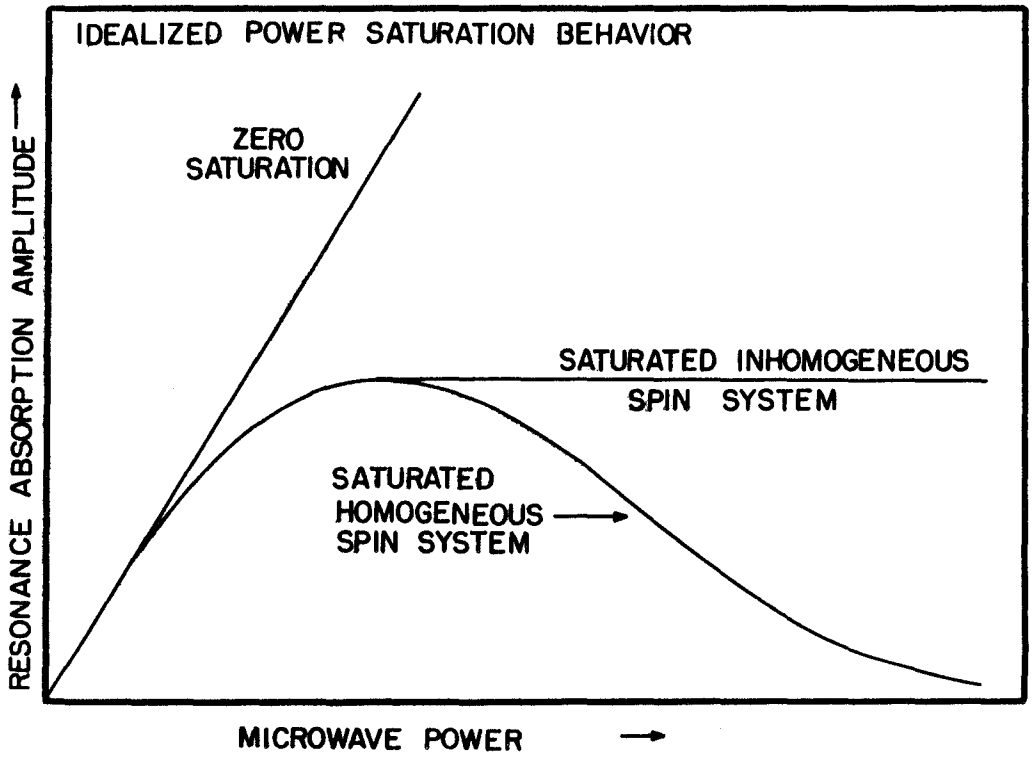

Fig. 7. Idealized power saturation behavior.

unpaired electrons. After each exchange a particular electron is still unpaired. The different local environments then result from different nuclear configurations (the nuclear configuration is "constant" as compared with electron relaxation times). 2) A particular unpaired electron becomes paired after an exchange. This case is well illustrated in Fig. 8. In the top picture each fluoranil has reacted to become a semiquinone radical (at 10^{-4} M concentration), in the middle picture only 1 in 20 fluoranils has become a radical, while at the bottom only 1 in 180 has reacted to become a semiquinone radical. The effect of exchange between the fluoranil semiquinone radical and the unracted fluoranil is clear.

g-Value Anisotropy. As noted above, the factor g appearing in the resonance equation represents the effective size of the magnetic moment being acted upon by the magnetic field. In crystal structures of less than cubic symmetry, the value of g can vary as the direction of the magnetic field is varied with respect to the crystal. Why this is so will be mentioned briefly below. The point we wish to make here is that in amorphous or polycrystalline materials an anisotropic g-value can produce quite broad asymmetric absorptions.

As an example of such an effect we can take the resonance of the copper in the protein complex ceruloplasmin (Fig. 9). The extremes in g-value are probably associated with the asymmetry of the molecular field around the copper. In a polycrystalline material there will be contributions from all g-values between extremes. Assuming tetragonal symmetry (8), the probability of H being parallel to the symmetry plane is twice that of its being perpendicular to this plane. The parallel configurations will therefore contribute more to the resonance absorption, and it becomes asymmetric. The spectrum resembles that of a frozen solution the copper-histidine complex.

This broadening mechanism differs from the others discussed in that its effect is directly proportional to the applied field. Working in two different applied fields will distinguish this type of asymmetry from other possibilities.

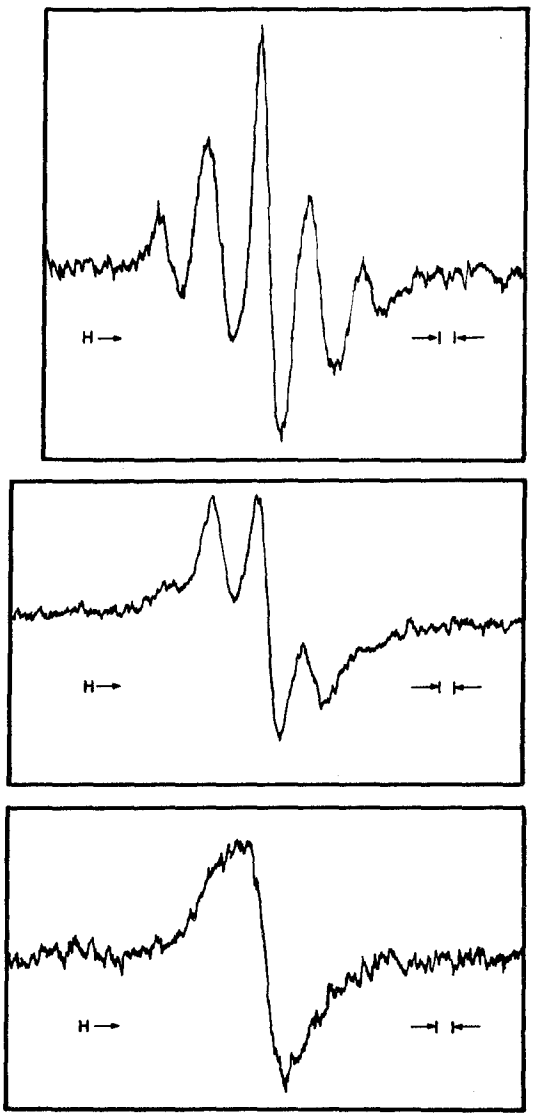

Fig. 8. The effect of electron exchange on the epr spectrum of 10^{-4} molar fluoranil semiquinone in 90% tetrahydrofuran -10% acetonitrile. The spectra were produced by reacting 0.005 molar NaI with 0.005 (top), 0.100 (middle) and 0.900 (bottom) molar fluoranil at -75°C. The scale magnitude of one gauss is indicated. (7)

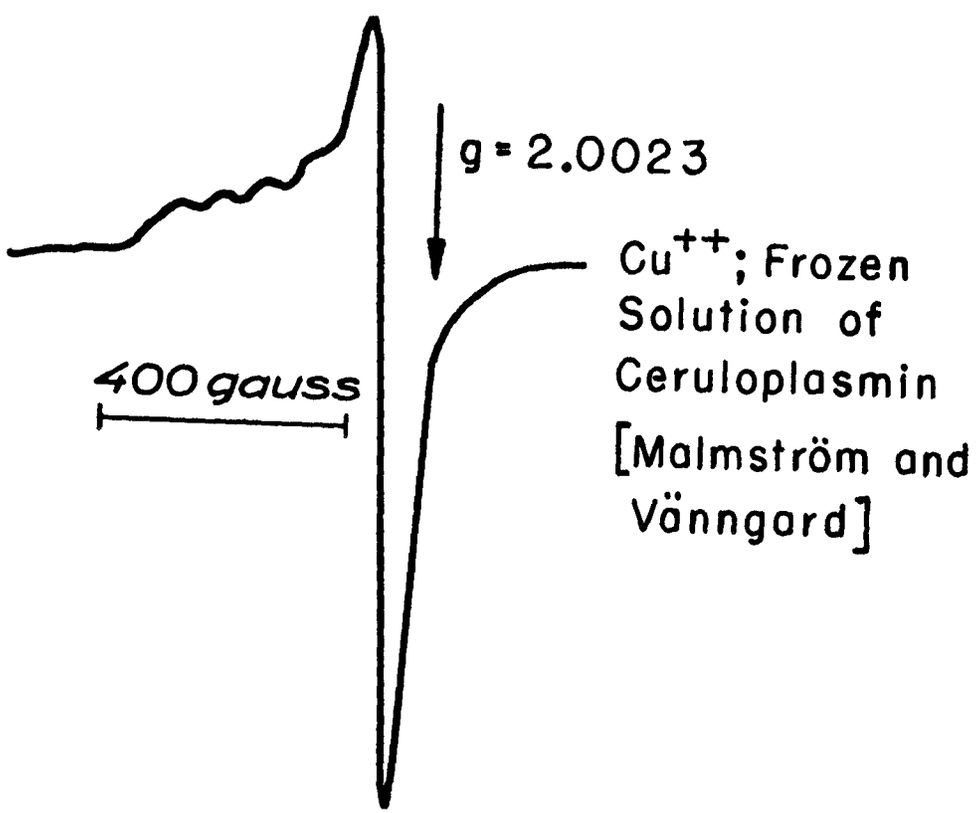

Fig. 9. The epr spectrum of Cu^{++} in frozen solid ceruloplasmin. T = 77°K. Magnetic field increases from left to right. (After 8)

Lifetime Broadening (Relaxation Broadening). As the lifetime, T_1, of a spin state becomes very short, the energy of that state should, according to the uncertainty principle, become correspondingly uncertain. In the extreme of very short T_1's ($\sim 10^{-11}$ sec) the resonance may go unobserved because of its width. The remedy in this situation is to lengthen T_1, usually by lowering the temperature. Although this effect can be important for conduction electrons, and for transition metal ions under certain circumstances, it is not generally important for free radicals.

E. g-Values.

Whether or not structure is resolved one can measure the g-value for the resonance. Experimentally this requires measuring, simultaneously, the strength of the magnetic field at which resonance occurs and the frequency of the microwave source.

The value of g differs from the "free spin" value (2.0023) because the electronic state has some degree of orbital angular momentum associated with it. The electron, as a magnetic moment, interacts with the magnetic field produced by the electron, as an electric charge, moving in an orbit. This interaction is called the spin-orbit interaction, and it is characterized by the relation

$$\mathcal{H}_{so} = \lambda \vec{L}\cdot\vec{S}$$

where L is the orbital-angular momentum quantum number, and λ is the spin-orbit coupling constant. This perturbation mixes states of higher energy and perhaps different symmetry properties with the ground state. When the Zeeman energy levels are calculated using the new (admixed) wave functions it is found that their separation has been altered by the perturbation. Also, their separation may be anisotropic with respect to the magnetic field direction because the perturbation has mixed in states of different symmetry. The effect, from the point of view of the resonance experiment, is to shift the g-value. The magnitude of the shift in g-value (from 2.0023) may be roughly approximated as $|\Delta g| \sim \frac{\lambda}{\Delta}$ where Δ is the energy separation between the ground and the first excited state.

$|\Delta g|$ is very small for organic free radicals. Blois (9), using sophisticated methods, has been able to establish some correlation between g-value and molecular structure or chemical substituents on a given structure. Some of his results are shown in Fig. 10. Most laboratories are not equipped for such refined measurements.

Values of $|\Delta g|$ as high as 2 or 4 have been observed in transition metal ions. (10, 11, 12) For a particular ion $|\Delta g|$ will depend very strongly on the strength of the molecular or crystal fields, and on the symmetry of the site.

g-Values as aids to identification can be useful if they are supported with independent data. This data could be in the form of spectrophotometric observations, chemical analyses, etc.

F. Thermal Relaxation.

The concept of thermal relaxation processes has been mentioned several times. Any process which changes magnetic to thermal lattice energy is such a process. A time characteristic of such a process can be defined in the following way. A spin system with a unique temperature T_s is not in thermal equilibrium with the lattice at temperature T_L ($< T_s$). At a certain time the perturbation keeping the spin system at T_s is removed. The spin system then returns to thermal equilibrium (i.e., to the lattice temperature) according to the expression $\exp(-t/T_1)$. T_1 is the spin-lattice relaxation time. This time is characteristic of the environment of the spin system, and will limit its rate of absorption of microwave power.

T_1 may be measured by continuous or transient methods. The amplitude of the resonance signal as a function of applied microwave power can be determined. As noted in Fig. 7, the shape of this curve is dependent upon whether the spin system is homogeneous or inhomogeneous. But given the type of system, the shape of the curve is determined by the magnitude of the product $H_1^2 T_1 T_2$. T_1 can thus be determined if T_2 and H_1 are known. (13) The transient method makes more direct use of the above definition of T_1. In this method the spectrometer is adjusted

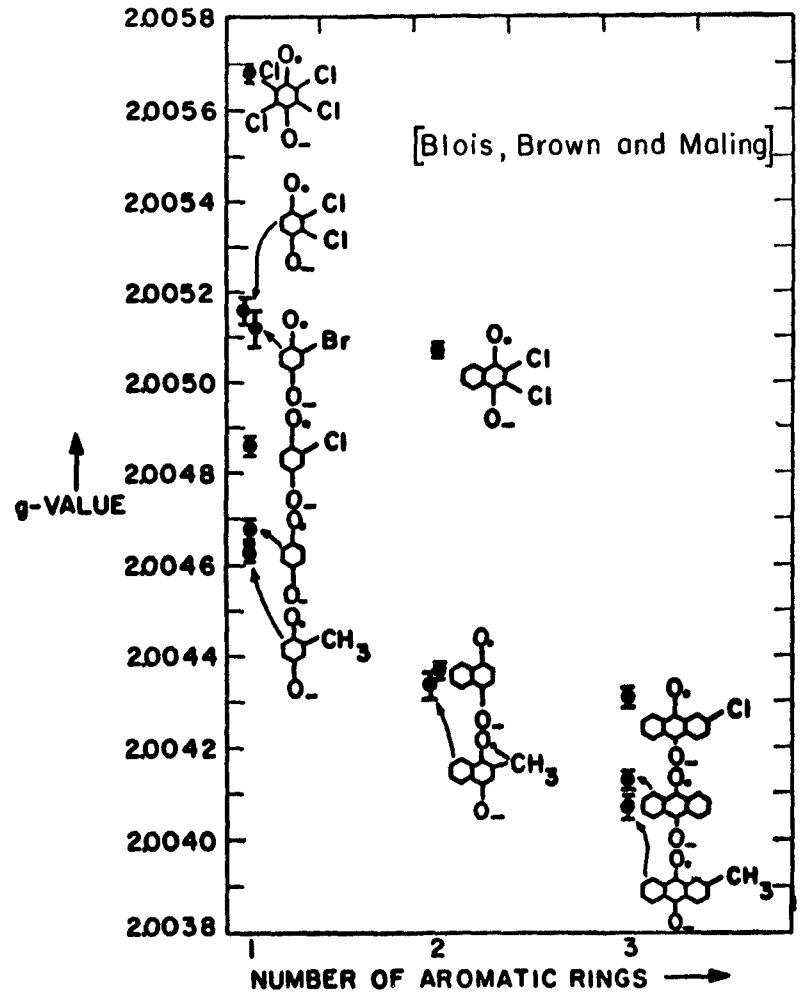

Fig. 10. g-Value as a function of the number of aromatic rings for some substituted benzosemiquinones. (After 9)

so that the amplitude of the resonance line is continuously observed. A short, intense burst of microwave power drives the system from equilibrium. The return to equilibrium is followed. See Fig. 11. (14)

G. Miscellaneous Measurements.

Even though a resonance line displays no resolved structure, there is one technique available for deciding which nucleii are coupled to the resonating electrons. The line must be inhomogeneously broadened in the sense that it is made up of unresolved components, and the relaxation times must be long. The technique, called "electron-nuclear double resonance" (ENDOR), is due to Feher (15) and is depicted in Fig. 12 for S = 1/2, I = 1/2.

As in the transient determination of T_1, the spectrometer is adjusted so that the electron spin resonance amplitude is continuously observed. This resonance is partially saturated. Then, while observing the amplitude of the electron resonance a second high frequency magnetic field is applied to the sample. This frequency is in the range of nuclear transitions (0 → 100 mc/s). Assume that while this frequency is being swept, one passes through the resonance of a nucleus coupled to the electron via the contact interaction, $A\ \vec{I}\cdot\vec{S}$. Inducing the nuclear transitions changes the population of the corresponding electronic levels. The latter change is reflected in the resonance amplitude being observed. ENDOR effects will be observed when

$$h\nu_I = 1/2\ A \pm \gamma_I H_z,\ (A >> \gamma_I H_z)$$

The ± sign comes from the fact that the top and bottom electronic levels are not split quite equally by the nucleii. Thus, one is able to solve for both A and γ_I. γ_I identifies the nucleus since in the absence of the unpaired electron the nucleus would resonate at frequency $h\nu_I = \gamma_I H_z$.

An example of the ENDOR technique is shown in Fig. 13 for phosphorus impurities in silicon. ν_I for P^{31} at about 3000 gauss is ~6 mc/s. Approximately twice this frequency is indeed the separation of the resonance peaks in Fig. 13a.

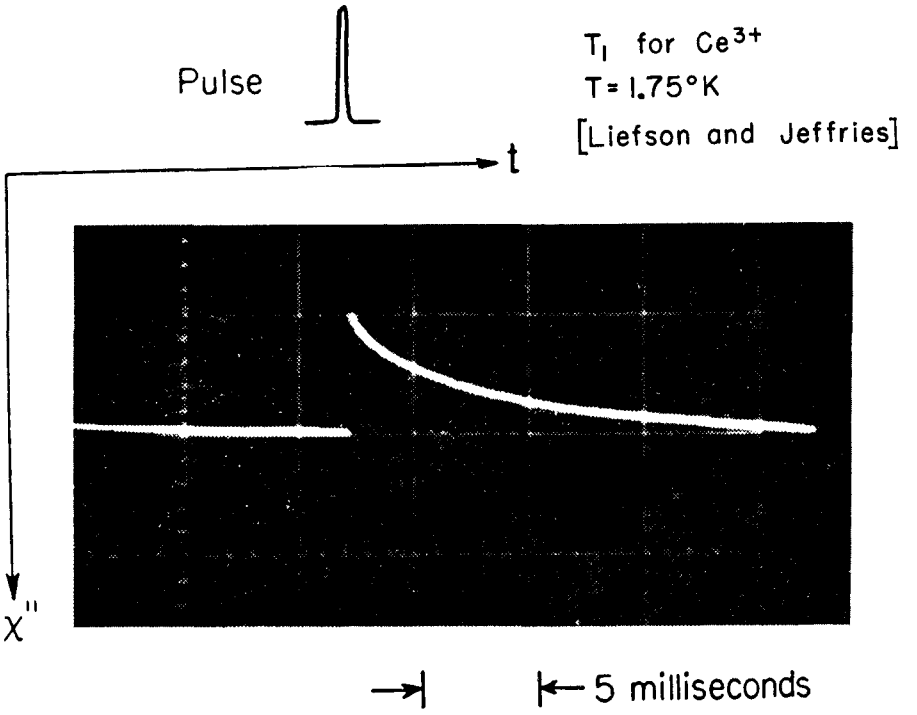

Fig. 11. Determination of T_1 using transient methods. Oscilloscope trace of recovery of Ce^{+++} absorption line following a saturating pulse of microwave power. (After 14)

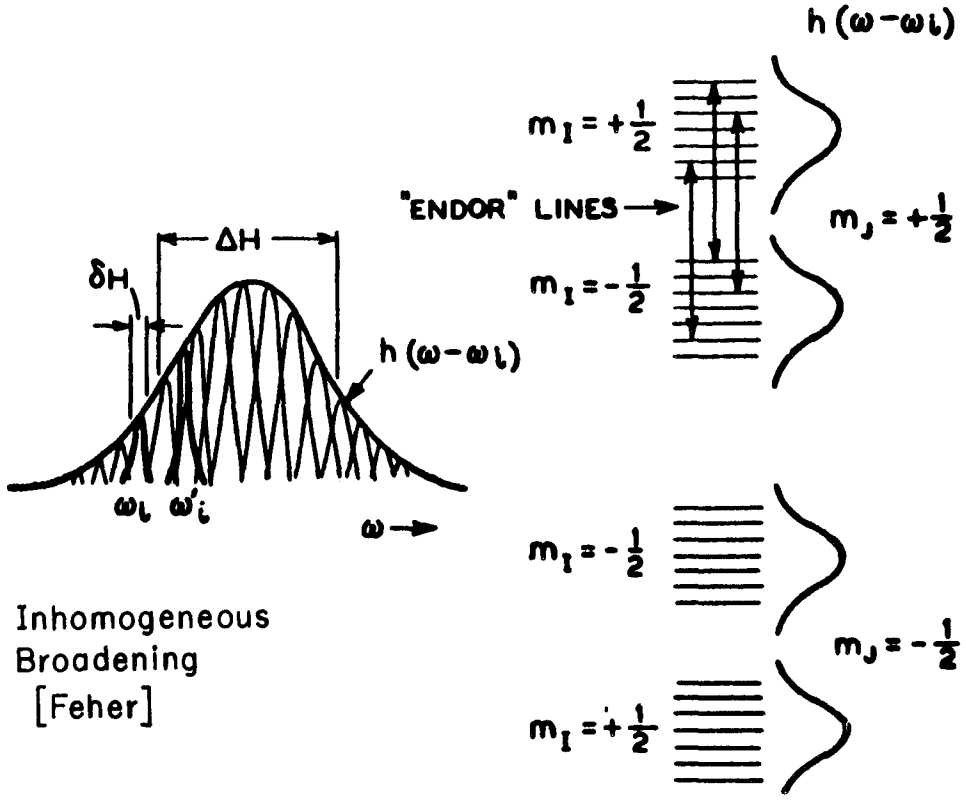

Fig. 12. Characteristics of an inhomogeneously broadened line. At left: the observed electron spin resonance line shape. One observes the envelope of many narrow resonance lines, each with slightly different resonant frequency, ω_i. At right: the energy level system which produces the observed resonance. Double resonance effects are observed in the electron resonance ($\Delta m_S = \Delta m_J = \pm 1$) when the nuclear transitions ($\Delta m_I = \pm 1$) are induced. (After 16)

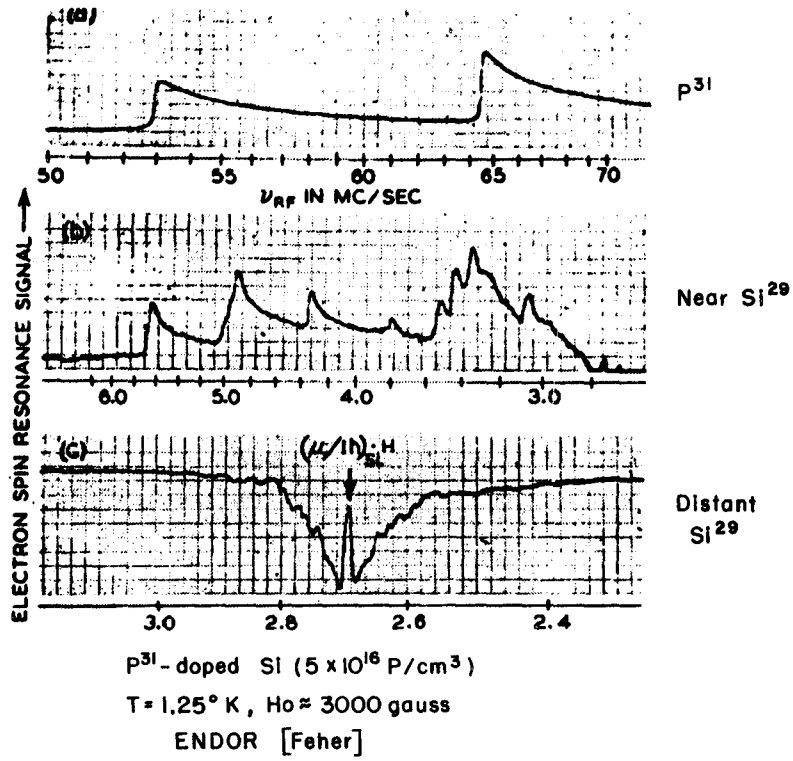

Fig. 13. Variation of the amplitude of the epr of phosphorus impurities in silicon as a function of the frequency of the "nuclear-transition" rf field. (After 15)

Long-lived triplet states have been observed using epr techniques. These states were first observed (17) using magnetically dilute, single crystals of naphthalene in durene. The transitions observed in the single crystal are depicted by the dashed lines in Fig. 14. Recently, van der Waals and de Groot (18,19) have discovered that the $\Delta m_s = \pm 2$ triplet transitions can be observed in glasses containing the excited molecules. This may make this technique applicable to biological samples in certain instances, although it shoud be noted that the probability of this transition is an order of magnitude less than $\Delta m_s = \pm 1$. The $\Delta m_s = \pm 2$ transitions observed in naphthalene-durene crystals are also shown in Fig. 14, as well as the anisotropy of the energy level system as H is varied with respect to the naphthalene molecule. The $\Delta m_s = \pm 2$, $g = 4$ resonances observed in naphthalene containing glasses are shown in Fig. 15. The $\Delta m_s = \pm 2$ transitions are allowed for H_1 both parallel and perpendicular to H_z.

H. Control of External Factors.

Most of the parameters mentioned can also be determined as functions of the physico-chemical and "biological" environments of the sample. In fact, it is from such functional dependences that most can be learned. Many variables immediately come to mind. Temperature, wavelength of light (in photo studies), ambient atmosphere, etc., would fall under the first category. Working with such things as mutants, selective extractions and simplified systems, selective inhibitors, etc., would fall in the second.

III. BIOLOGICAL APPLICATIONS.

We have listed the parameters characteristic of a resonating electron system. We now ask to what degree these measurements have been applied to biological systems, and where applied, to what extent they have helped to resolve problems. It will become immediately obvious that at this stage of their application to biological systems these measurements of resonance parameters, in and of themselves, are relatively impotent in solving major biological problems. They do, indeed, supply

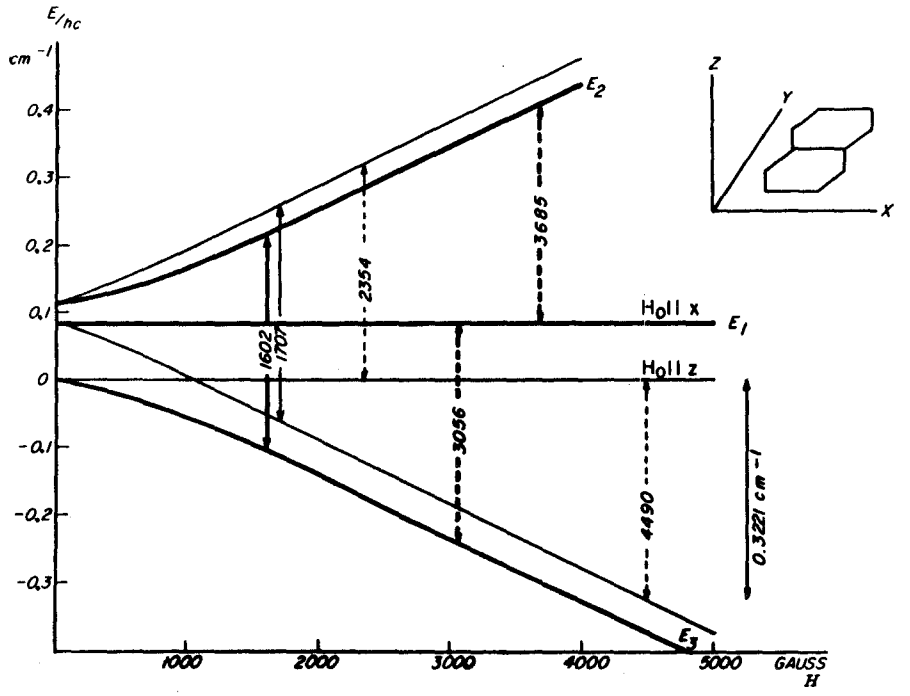

[Van der Waals and de Groot]

Fig. 14. Relative energies of the components of the lowest triplet state of naphthalene as a function of magnetic field. Heavy lines: magnetic field along x axis. Thin lines: Magnetic field along z axis. The dashed transitions indicate those observed by Hutchinson and Mangum (17). Solid transitions observed by van der Waals and de Groot (18). (After 18)

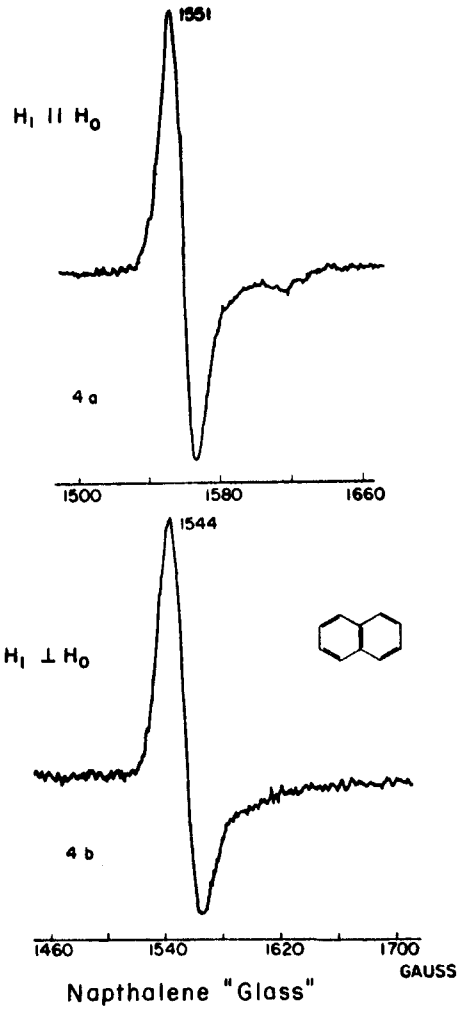

Fig. 15. The epr spectra of $\Delta m_s = \pm 2$ transitions of naphthalene in a rigid glass. (a) H_1 parallel to H_z. (b) H_1 perpendicular to H_z. T = 77°K. (After 19)

much new and unique data, but these must be supported by many kinds of physico-chemical-biological information before they can be made meaningful in biological terms. This situation will change. As specific radical sites are identified, and specific reaction mechanisms are proposed, the strictly physical parameters of the resonance will become more important in deciding between possibilities. Thus, while the first reported applications of epr techniques to biological systems dealt with essentially whole systems (20,21,22), the emphasis of late has been toward the simpler, better defined systems. Our review of applications will start with these and proceed to the more complex or whole systems.

A. Simplified Systems.

Many molecules of basic biological interest have been investigated using epr techniques. Some of these have already been mentioned in Section II as examples of what one observes. The spectrum of Mn^{++} ion (Fig. 4) is observed in some biological systems (see below). The metallo-derivatives of the widely distributed porphyrin (and the related phthalocyanine) type structure are being studied (Fig. 6) (6, 10).

A large number of the simpler semi-quinone type radicals have been observed as intermediates in oxidation-reduction equilibria (5, 23). Blois et al. (9) have recorded the g-values of many of these. One example was given in Section II for halogen substituted para-benzoquinones (Fig. 5). Another is given in Fig. 16, for the semiquinone of coenzyme Q. The distribution of the unpaired electron on the molecule is uniquely determined by the resolved structure of the resonance. The resonance of Fig. 16 is, of course, for coenzyme Q semiquinone radical in solution. The resonance of the same radical in a solid would lose much of its detail.

An example of what one usually encounters, a radical situated in a solid structure, is given in Fig. 17, (25), the bottom curve. The solid here is multi-crystalline choline chloride, a compound of great biological interest. Radicals were introduced into the solid by irradiation with 4.5 -mev electrons, and a peculiar solid state

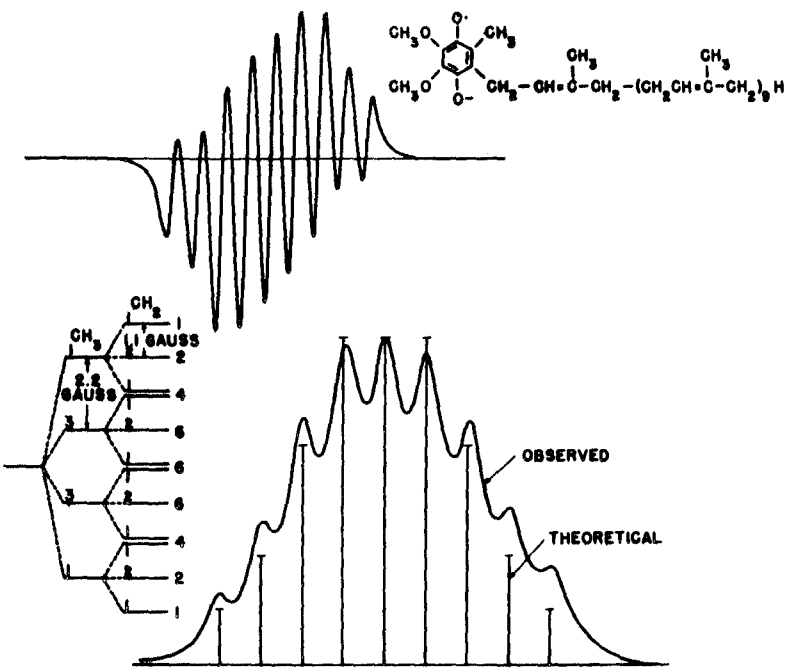

The e.s.r. spectrum and line assignment for the semiquinone free radical of Coenzyme Q_{10}

Fig. 16. The epr spectrum and line assignment of the semiquinone free radical of coenzyme Q_{10}. (After 24)

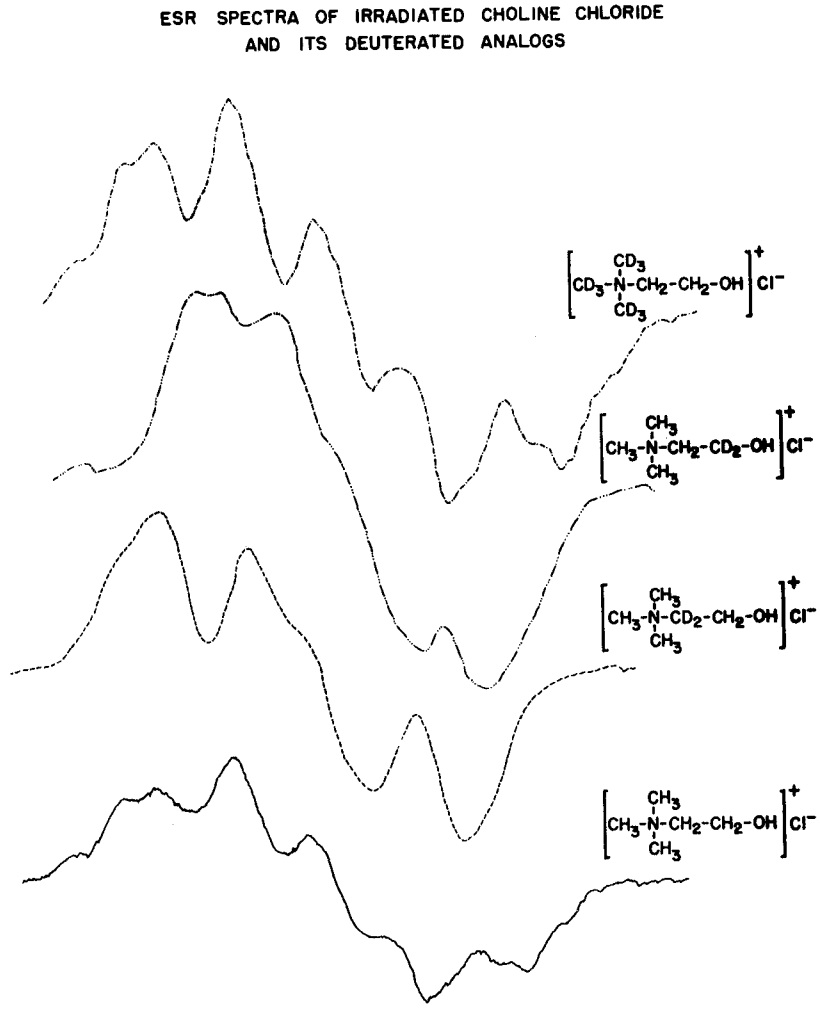

Fig. 17. The epr spectra of irradiated choline chloride and its deuterated analogs. Polycrystalline material: 4.5 mev electron irradiation. (After 25)

radical reaction was observed. With incomplete resolution of the resonance structure identification of the radical environment becomes considerably more difficult. The epr technique must be supplemented. On the basis of the results obtained from selective deuteration of the solid (top three curves of Fig. 17), it was concluded that the radical was associated with the structure: $CH_2.CH_2OH$. Wertz et al. (26) have also used deuterium substitutions to aid in identification of the radical intermediates of the auto-oxidation of 3,4-dihydroxyphenylalanine.

B. Intermediate Systems.

Nucleic Acids. Broad, intense resonance absorptions have been observed in nucleic acid-albumin systems (27, 28, 29). Under the correct conditions of pH, ionic strength, and protein content, energy absorption occurs at all fields between zero and 6000 gauss (with g = 2 at $\sim$ 3300 g), Fig. 18. Recently, essentially the same type of epr spectra have been obtained using Fe^{3+} treated resins (Fig. 19) (30). From estimates of the area under these absorption curves the spin concentration is estimated to be $10^{20} \rightarrow 10^{21}$ spins/gram. In arriving at this number it was assumed that the energy is absorbed by a system of uncoupled electrons (S = 1/2). Bliuminfel'd et al. (29) have reported that for the nucleic acids, the resonance absorption suddenly and completely disappears when the temperature is reduced below 80 to 100°K. Blois (31) could not bring this effect about by lowering the temperature of a sample of DNA to 77°K. Such a temperature dependence, if it really exists, is common to materials known as anti-ferromagnetics. The presence of coupled spin systems in such materials would have several implications (32). The estimate of the spin concentration could be one or more orders of magnitude too high. This results from the fact that the distribution of the spin population among the various magnetic levels is no longer set by the Boltzmann factor (as was assumed in deriving the expression relating area under absorption curve to spin concentration), but by the energy of the magnetic interaction, as in

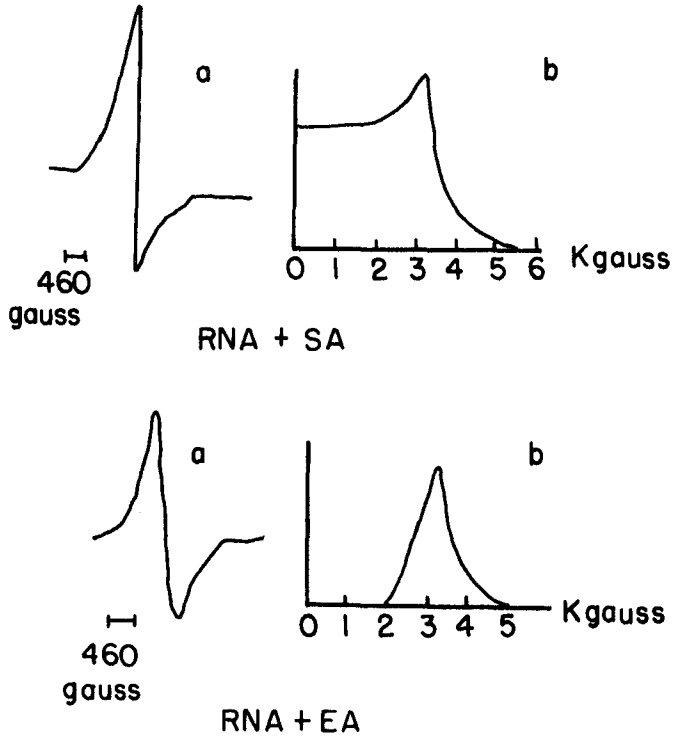

Fig. 18. The epr spectra of RNA and egg albumin (EA) and of RNA and serum albumin (SA).
Conditions: RNA + SA - 21 ml of 1% solution of serum albumin, 45 ml of 0.2% solution of RNA, 12.6 ml of N-acetate buffer (pH = 4.0) containing 5.6% NaCl.
RNA + EA - 24 ml of 1% solution of egg albumin, 45 ml of 0.2% solution of RNA, 13.1 ml of N-acetate buffer (pH = 4.0) containing 5.6% NaCl.
(After 29)

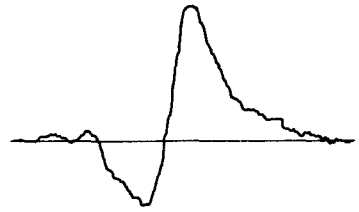

SALMON SPERM DNA
(LYOPHILIZED)

(1a)

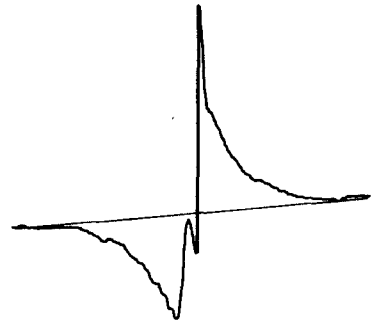

CALF THYMUS DNA
(LITHIUM NUCLEATE)

(1b)

SALMON SPERM DNA
(SUPERNATANT) (120°K)

(1c)

WHOLE SALMON SPERM
(LYOPHILIZED)

(1d)

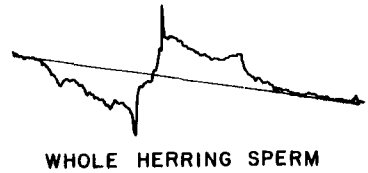

WHOLE HERRING SPERM
(LYOPHILIZED)

(1e)

CONTROL
(RESIN AS OBTAINED)
(GAIN 250x)

(1f)

RESIN + Fe^{+++}
x 1
(GAIN 250x)

(1g)

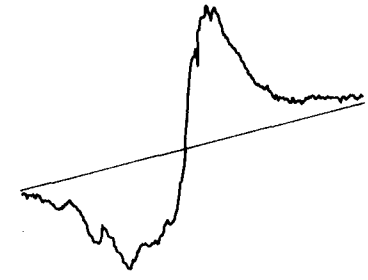

RESIN + Fe^{+++}
x 10
(GAIN 250x)

(1h)

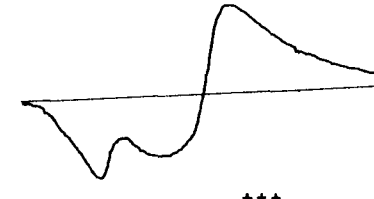

RESIN + Fe^{+++}
(SATURATED)
(GAIN 25)

(1i)

1500 GAUSS

ferromagnetics. The elements of the coupled system are probably transition metal ions (as impurities or normal constituent elements), as these are involved in all known cases of coupled systems. Their concentration is sufficient to explain the results in all cases if a coupled spin system is allowed (32). Introducing the idea of coupled spin systems may explain the high spin concentrations reported, but it opens another question: i.e., what properties do the nucleic acids have that promotes the coupling of the transition metal ions at such extreme dilutions?

Ionizing Radiations. A great deal of work is being done on the effects of ionizing radiation on biological materials. These studies have been made on the trapped radicals produced, so solid or highly viscuous sample materials are generally used. This in turn makes identification of the radical site difficult. The complexity of the problem was realized early in these studies, so much of the work that has been reported has been of a "cataloging" nature. This consists, for example, of studying the epr spectrum obtained from irradiation of each of the constituent bases of the nucleic acids in preparation for studying the irradiation of the whole molecule. An example of this approach, taken from the extensive radiation damage studies of Gordy (33), is shown in Figs. 20, 21 and 22. The sugar and base constituents of RNA and DNA, obtainable from the acids by hydrolysis, are irradiated as evacuated dry powders at room temperature. After giving each constituent a radiation dose of approximately 5×10^6 r from a kilocurie Co^{60} γ-ray source, its epr spectra were recorded. Fig. 20 shows the results obtained from the pyrimidine base constituents, while Fig. 21 shows the results obtained from the constituent sugars. Thymine (5-methyl-uracil) and 5 methyl-cytosine exhibit markedly different spectra. The two molecules differ only in the 4 position where thymine has an OH group while 5-methyl-cytosine has an NH_2 group. When the epr spectra of the 4 molecules of Fig. 20 are compared, it is

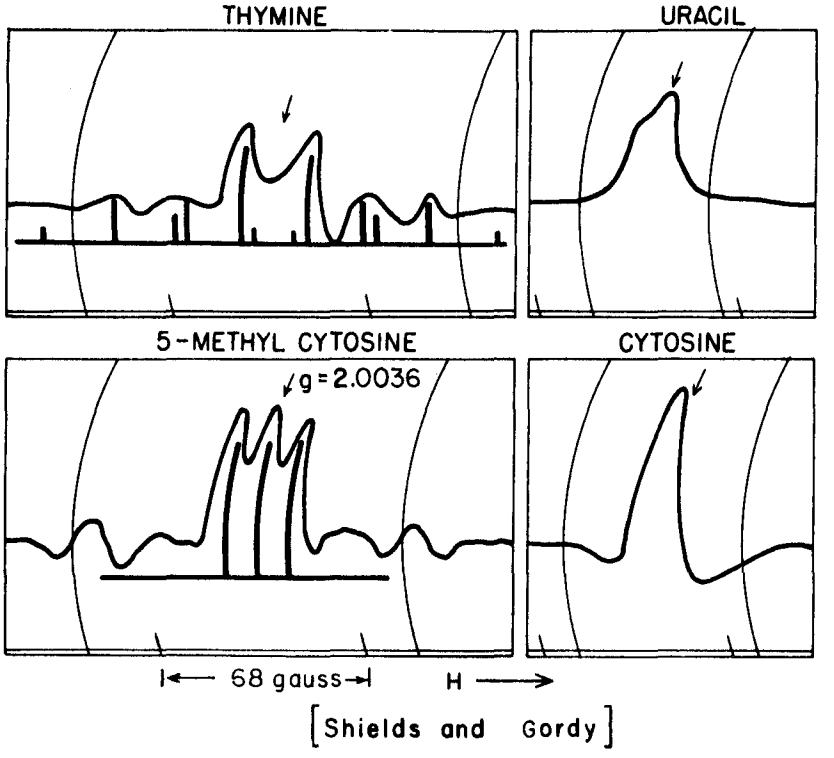

Fig. 20. The epr spectra for γ irradiated pyrimidine bases. The curves are second derivatives of the absorption curve. The bars represent theoretically possible patterns for the fine structure. Irradiated at room temperature as dry powders under vacuum. Dose = 5×10^6 r from a kilocurie Co^{60} γ-ray source. Epr ran on dry powders at room temperature. (After 33)

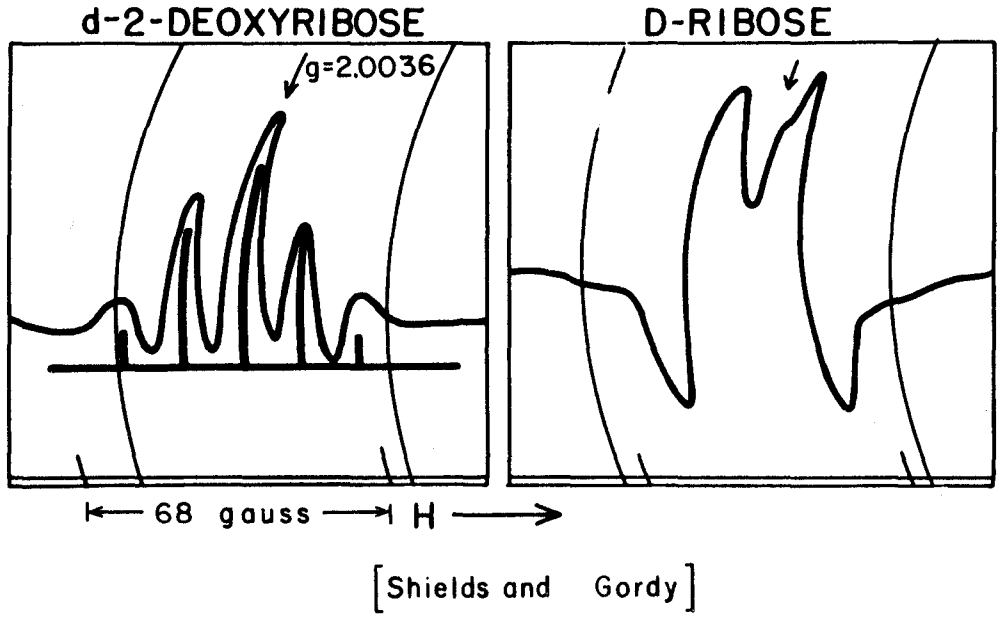

Fig. 21. The epr spectra of γ irradiated d-2-deoxyribose and d-ribose. Conditions as in Fig. 20. (After 33)

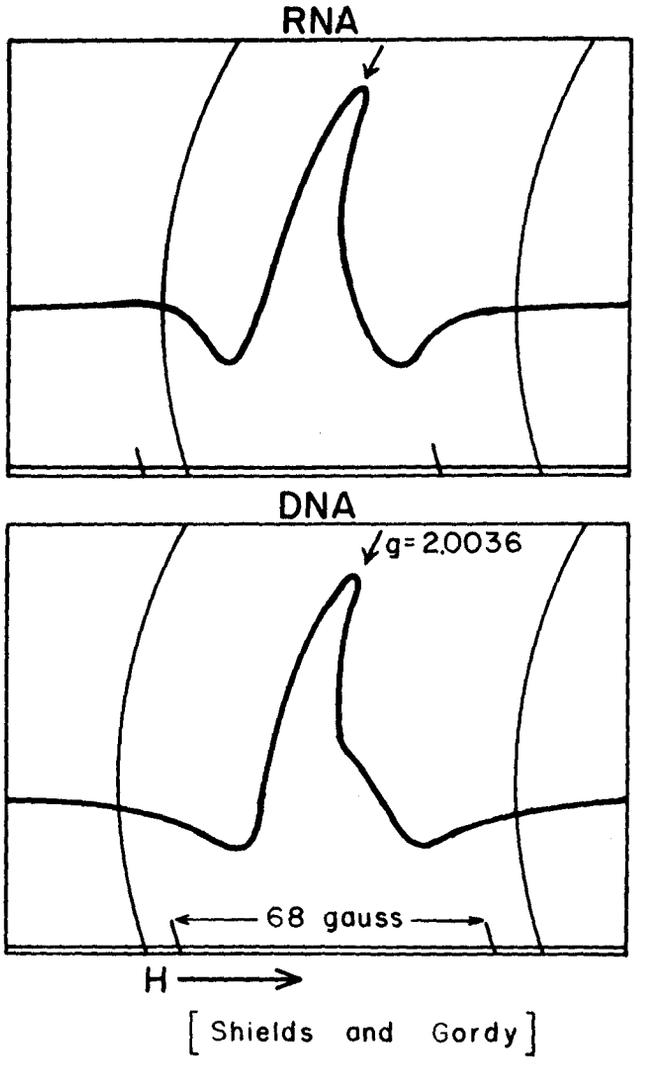

Fig. 22. The epr spectra of γ irradiated RNA and DNA. Conditions as in Fig. 20. (After 33)

seen that the presence of the methyl protons and the N^{14} on the 4 position of cytosine have marked effects on the results. In the sugar constituents (Fig. 21) the epr coupling seems to be predominately to a spin 2 system in one case and to a spin 1/2 system in the other. In none of these cases could a definite assignment of the radical site be made. After recording the epr spectra of the remaining constituent bases, DNA and RNA are finally irradiated and their epr spectra recorded. The resulting spectra (Fig. 22) can be identified with that of none of the constituents. In shape they resemble cytosine most. Here, however, there is a discrepancy in g-value. Thus, it is seldom, even in relatively simple systems, that one identifies the molecular group upon which the radical resides, let alone its detailed environment in the group.

There is a quest running through the work involving ionizing radiation for chemicals which will mitigate the biological effects of the radiation. As is known, several such chemicals have been found, notably compounds containing sulphur and some amines (e.g. cystine, cysteamine). In an epr experiment the possibility for such protection is evidenced in two ways. 1) By the appearance for example, of only the resonance of irradiated cystine in the epr spectra of complex structures containing cystine as only one of many possible radical sites. 2) By the partial prevention of radical formation (i.e. a decrease in epr amplitude in cases where the protective agent has been added). Apparently, the sulphur group is able to absorb the energy of the ionizing radiation, leaving the biological function of the protein or other polymer unimpaired.

It has generally been concluded that the energy of the incident radiation is chemically transferred (involving the making and breaking of bonds) to the S group. (34, 35) The protective effect of cysteamine on bovine serum albumin exposed to γ rays at liquid nitrogen temperature (Fig. 23) (34) seems to indicate that the energy alone is transferred. In this system the SH groups are not reacting in an ordinary chemical manner, i.e. by nuclear migration, because of the low temperature.

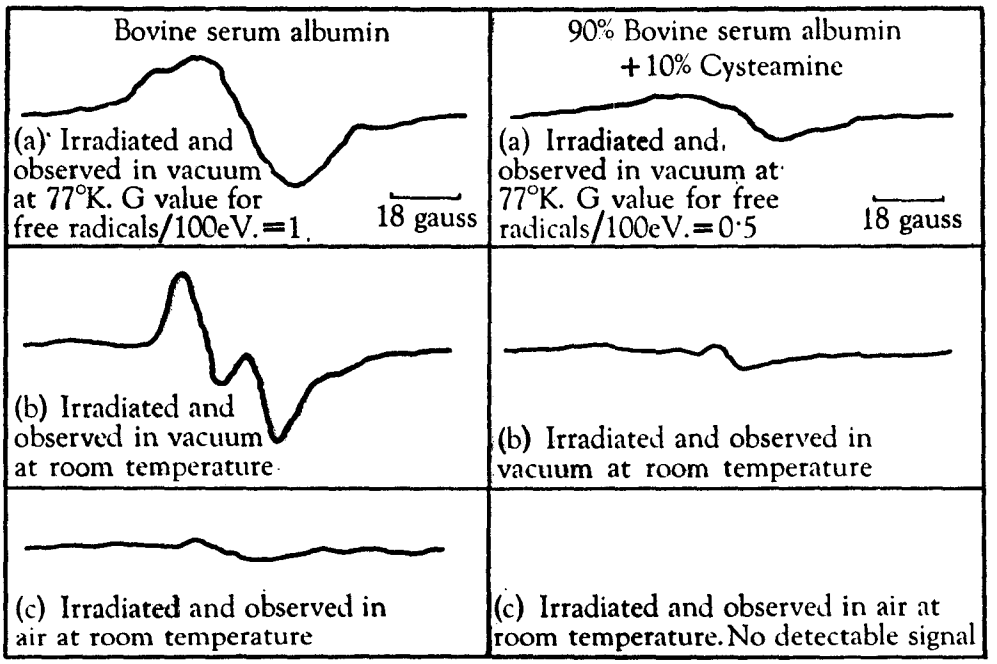

Fig. 23. The epr spectra of γ irradiated "protected" and "unprotected" bovine serum albumin. Dose = 5 M rads at 750 Krads/hr. (After 34)

Visible Radiation. Visible light quanta are sufficiently energetic to produce unpaired electrons in some systems. We refer, of course, to systems related to photosynthesis. Several studies have been made on relatively simple systems, involving pigment molecules active in photosynthesis.

Terenin and Holmogorov, in a recent study on "crystalline" chlorophyll (a + b) in vacuo (36) have observed two overlapping resonance curves (Fig. 24). One ($g = 2.0035$, half width = 11 g) ("a" in Fig. 24), is always present. The second ($g = 2.0030$, half width = 7 g) is light induced in the presence of an electron acceptor. Water vapor (at 18 mm Hg pressure) and p-benzoquinone molecules (at 2×10^{-2} mm Hg) are both effective as acceptors, although the rise and decay kinetics of the quinone induced photo signal are much the slower of the two cases.

A dependence of epr signal on the presence of H_2O has been observed by Anderson (37) in an acetone extract of spinach chloroplasts. The extract was evaporated to dryness and tested (in vacuo) for the presence of a photo induced epr signal. No signal (either in the dark or light) was observed. However, when water vapor was admitted to the system narrow ($\sim$ 4 gauss wide) photo induced signals were observed, whose rise and decay times were much shorter than those reported by Terenin. These short times seem to be dependent upon the presence of as yet unknown components. The amplitude of the signal induced as a function of the amount of water present (Fig. 25). If these observations survive more detailed investigation, and do indeed correspond to a photo-electron transfer between water and chlorophyll, they may point the way to an understanding of the more complex systems we will discuss later.

Krasnovskii, et al. (38) have thoroughly studied the photo oxidation of ascorbic acid in pyridine solution, using chlorophyll as a sensitizer. The epr observation is on a free radical form of oxidized ascorbic acid. This radical

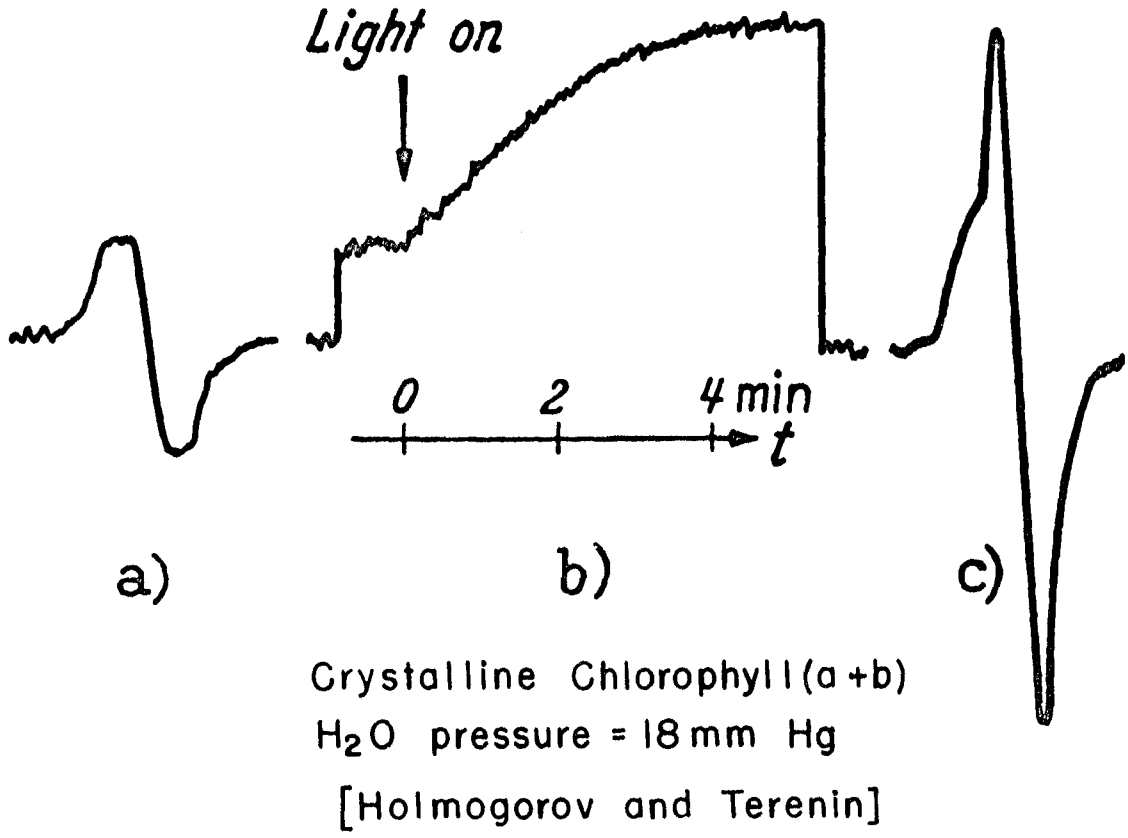

Fig. 24. Light induced epr in "crystalline" chlorophyll (a + b) in vacuo in the presence of water vapor. (a) dark, (b) response to light, (c) superimposed dark and light signals. (After 36)

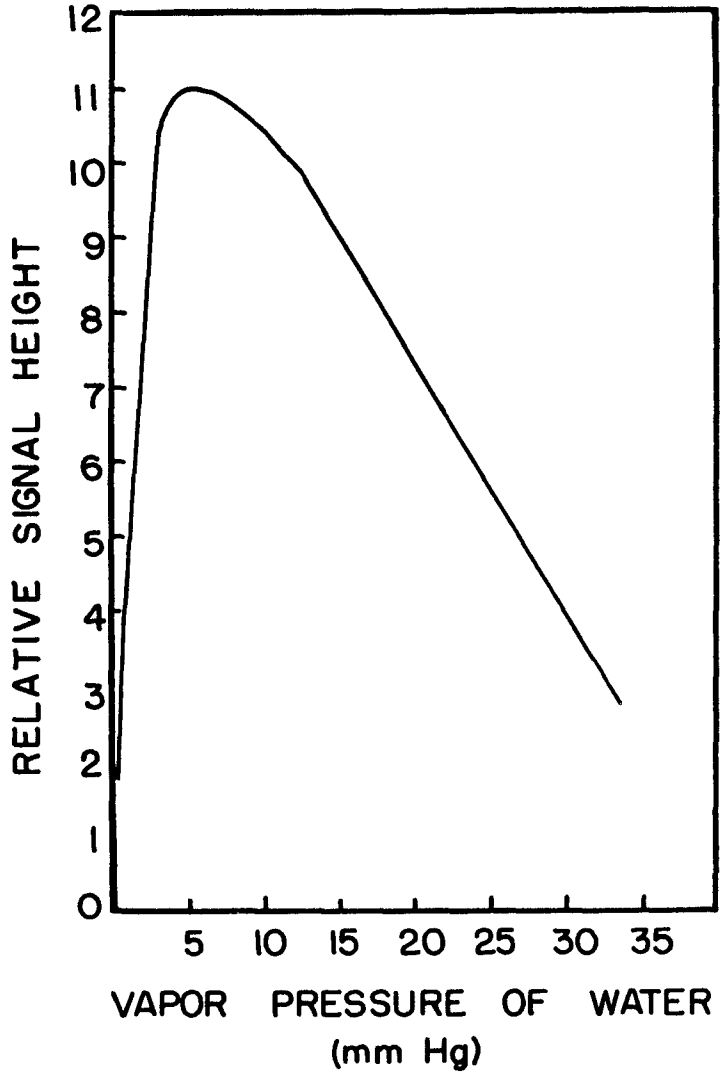

Fig. 25. The light induced epr amplitude in an acetone extract of spinach chloroplasts as a function of the pressure of water vapor present. The extract was evaporated to dryness and evacuated before admission of water vapor.

produced a resonance which is a doublet with separation 1.8 gauss at g = 2.004. (This resonance will be discussed further in connection with photo induced epr signals in whole photosynthetic systems).

Enzymatic Oxidation-Reduction. Enzymatic oxidation-reduction reactions have been followed in relatively simple systems. System simplicity is an important factor in identifying radical species. Free radical intermediates specifically identified with the substrate as well as the participation of transition metal ions in these reactions have been reported.

Yamazaki, Mason and Piette (39) have identified the free radical intermediates observed in a peroxidase system, as being the radical form of the substrate itself (ascorbic acid). This they did by independently forming the substrate radical. The kinetics of radical formation and decay were followed, using a stop-flow system which mixed their reacting substances (10^{-2} M ascorbic acid, 10^{-2} M H_2O_2, and 2 x 10^{-7} M peroxidase), and immediately injected them into the epr cavity. The spectrometer had been previously adjusted to observe the amplitude of the radical resonance as it formed and decayed. Thus, a continuous record of radical concentration is made. Some of their results are reproduced in Fig. 26. The radical concentration in the cavity rises in less than 0.010 sec. to $\sim 10^{-6}$ M/l, then decays, apparently in two steps.

A simplified dehydrogenase system has been employed by King, Howard and Mason (40). This consisted of a soluble succinic dehydrogenase in combination with various substrate concentrations. Their reaction components were combined at room temperature, and their epr spectra were taken at 77°K (Fig. 27). By observing the peak amplitude ratios as experimental conditions were varied, they were able to show that the signals observed at g = 2.01 and g = 1.94 were due to one magnetic species, while the resonance observed at g = 2.00 was due to another. The resonance structure shown in Fig. 27 is quite similar to one observed by Beinert and

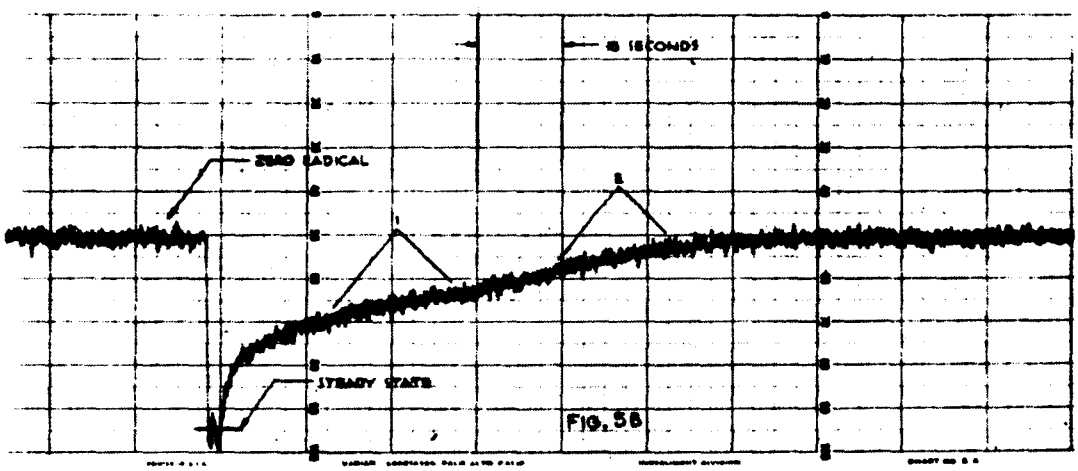

Decay of Ascorbic Acid Free Radical
[Yamazaki, Mason, and Piette]

Fig. 26. Decay kinetics of ascorbic acid free radical. The ascorbic acid, H_2O_2, peroxidase mixture is injected into the cavity at the sharp drop in the curve on the left. Time progresses toward the right. (After 39)

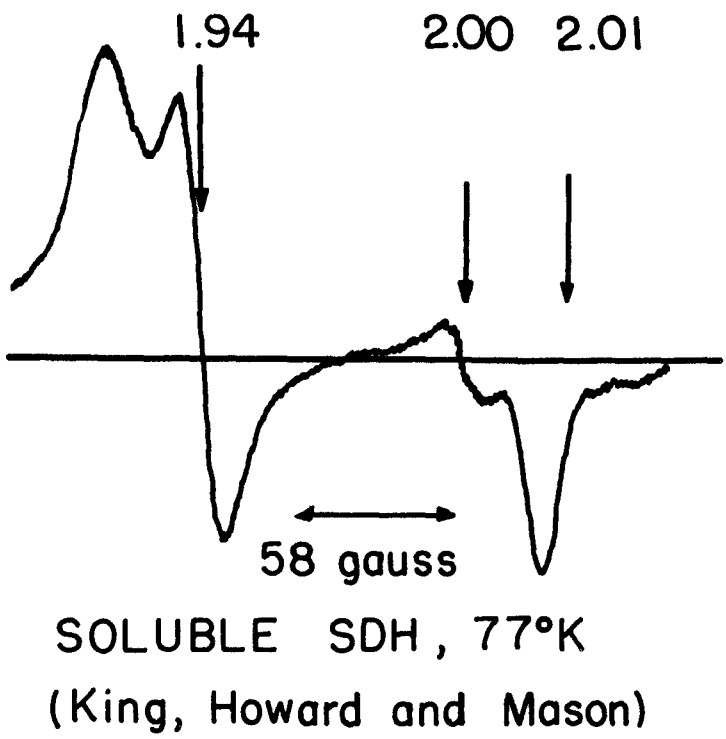

Fig. 27. The epr spectrum of soluble succinic dehydrogenase at 77°K. Conditions: 2.6 mg protein in 0.1 M phosphate buffer pH = 7.8: 5.8×10^{-2} M succinate: sample volume = 0.2 ml. (After 40)

Lee in a more complicated system (see below). Beinert and Lee attribute the resonance at g = 1.94, 2.01, to Fe^{++}.

Resonance absorption from transition metal ions has been reported in several enzymatic redox reactions; Beinert and Sands (41, 42) and Beinert and Lee (43) report Fe^{++} at g = 1.94, Fe^{+++} at g = 4.3, and Cu^{++} at g = 2.04 in their dehydrogenase systems (see below). Vanngard et al. (44) give g = 1.971 for Mo^{3+} or Mo^{5+} in an xanthine oxidase system. This resonance is relatively symmetric and 25 g wide, while that reported for Cu^{++} is very asymmetric and several hundred gauss wide (see Figs. 9 and 28). The identification of these transition metal ions as reactants in enzymatic redox reactions is not really on firm ground. Analogies have been drawn from spectrophotometric studies of the same systems, known resonance g-values in related compounds, or merely the known concentrations of transition metals present. As remarked in Section II, the g-values and g-value asymmetries will be strongly dependent on the particular local environment for a particular oxidation state of an ion. Iron in acidic ferrimyoglobin resonates at g = 6 when the external magnetic field is in the plane of the heme (11).

C. Biological Systems.

Enzymatic Oxidation Reduction. Beinert and Sands (41, 42) and Beinert and Lee (43) have investigated the enzymatic redox reactions associated with the mitochondrial electron transport system. Their systems have involved homogenates, mitochondrial, and submitochondrial preparations of beef heart. These studies have shown that changes of oxidation level of transition metal ions, as well as free radical intermediates, are involved. An example of their results is given in Fig. 28. To a small amount of submitochondrial particles from beef heart they added micromolar amounts of DPNH or succinate (A and B, respectively, in Fig. 28). These were allowed to reduce substrate at $0^{\circ}C$. for the periods of time indicated in the figure. At that point, chemical reactivity was stopped by

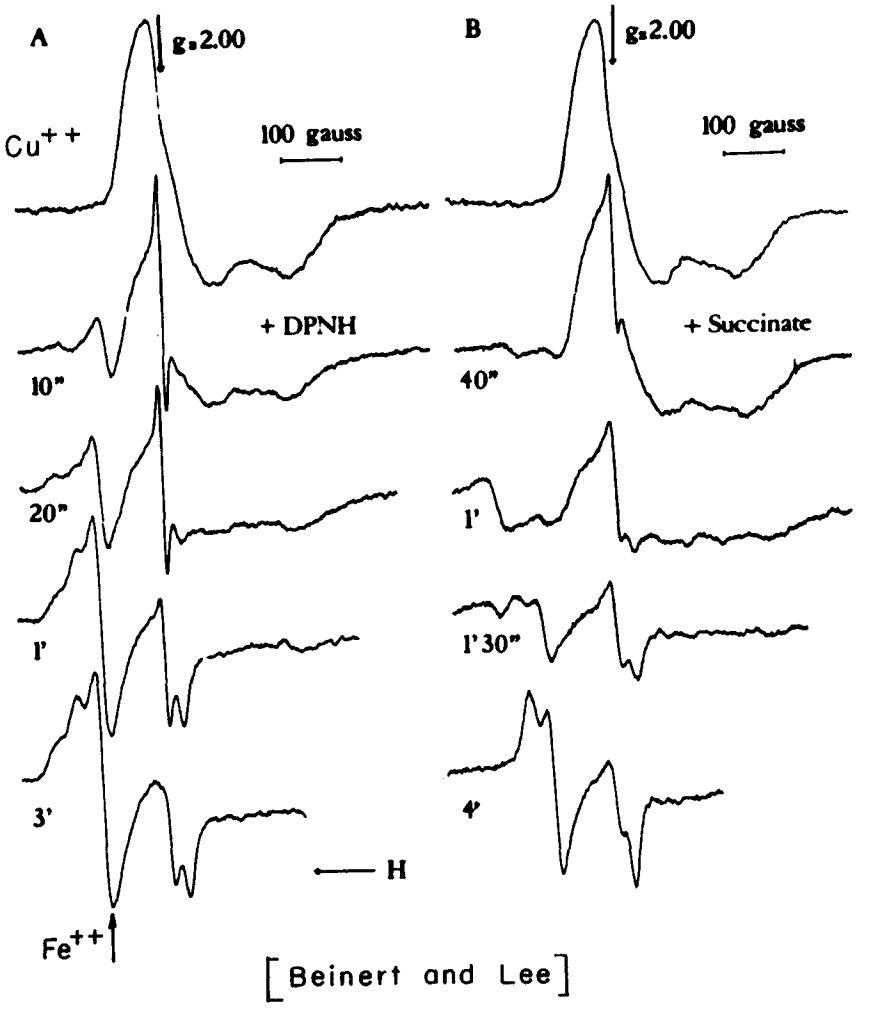

Fig. 28. The epr spectra of submitochondrial particles of beef heart as a function of the time enzymatic reduction by DPNH (A) and succinate (B) is allowed to continue at $0^{\circ}C$. Spectra taken at $-178^{\circ}C$. (After 43)

lowering the temperature of the preparation abruptly to -170°C. The spectra of Fig. 28 were then recorded. The kinetics of the various concentrations of magnetic species is quite involved. A Cu^{++} resonance disappears as a free radical signal appears and disappears while, finally an Fe^{++} resonance grows in. The bottom curve in either case is similar to the spectrum obtained by King, Howard and Mason (Fig. 27) in a simpler system.

Ionizing Radiation. In the epr observations of the effects of ionizing radiation on essentially complete biological systems, there are few regularities. One regularity is the frequent appearance of the epr spectrum of irradiated cystine as the total epr spectra of irradiated naturally occurring proteinaceous materials (45, 46). As discussed above, cystine is a compound which "protects" biological materials against ionizing radiation. The observed resonance is about 140 gauss wide, quite asymmetric, and appears near g = 2.00. Another regularity which occurs in the epr irradiation studies is the frequent appearance, as the total observed spectrum, of a symmetric doublet with splitting of 12 gauss and essentially the free electron g-value (45). This is attributed to an unpaired electron on an oxygen atom interacting with a hydrogen bonding proton on the adjacent polypeptide chain. The interaction is dipole-dipole. Thus oxygen can also act to accept ionization energy.

Visible Radiation (Photosynthesis). The ionization studies might be said to be suffering from too much detail - every system gives different un-interpretable results. On the other hand, the application of epr to photosynthetic systems could be said to be suffering from dearth of detail. Almost every system investigated yields a niggardly, rather narrow, single absorption line. (More recently two overlapping resonances have been observed in some systems. Others yield, still, the single line.) Thus, all conceivable tricks are being used to elucidate the nature of the radicals observed in photosynthetic systems.

Resolved fine structure has only seldom been reported in photosynthetic materials. Krasnovskii et al. (38) report a photo induced electron spin resonance doublet in photosynthetic material. Their results are reproduced in Fig. 29. The g-value for the resonance is 2.004 and the line splitting is 1.8 gauss. Using model photochemical reactions as a basis for reasoning, this group has attributed the photo induced doublet in the photosynthetic system to an oxidized form of ascorbic acid (see above). Commoner et al. (21, 47) have also reported a partially resolved structure in chloroplasts and Chlorella. This resonance is photo induced but decays away very slowly. It has a g-value of 2.005 and consists of 5 lines each separated by 6 gauss.

Another resonance with easily resolved structure which is observed in chloroplasts, some green algae and bacterial spores, is that of Mn^{++}. This resonance does not appear to be photosensitive. As shown in Fig. 4, the structure consists of 6 lines. The Mn^{++} concentration in these samples is as high as 10^{-6} to 10^{-5} molar.

Many people have resolved structure in photosynthetic systems in the sense that two distinct overlapping resonance lines have been resolved. (48, 49) One of these has already been mentioned, namely, the slow decaying signal with some structure, observed at g = 2.005. The second resonance (also photo induced with fast rise and decay times) is narrow ($\sim$ 10 gauss wide) and has a g-value of 2.002. To resolve these signals small modulation amplitudes and high instrument sensitivity are required. Under conditions in which the two resonances are easily resolved in green algae, there is still only one narrow line resolved in the photosynthetic red bacteria Rhodospirillum rubrum.

The derivative of this single line is shown in Fig. 30. This resonance may be classified as inhomogeneous. Its width does not change as a function of microwave power incident on the sample. It saturates approximately as does

10 oersteds

1) Triticum vulgare

2) Hordeum vulgare
Room Temperature

[Krasnovskii, et al]

Fig. 29. The epr spectra of illuminated cereal leaves. These signals are presumed by the authors (38) to be due to ascorbic acid free radical.

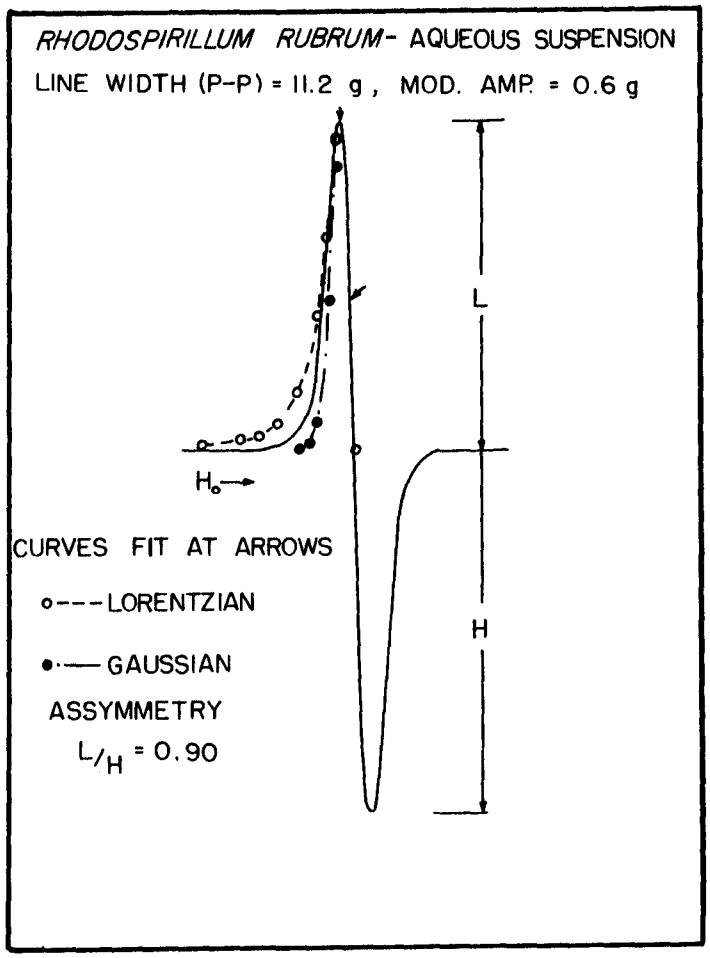

Fig. 30. Line shape analysis of the epr spectrum of Rhodospirillum rubrum in aqueous suspension at room temperature.

the signal in Rhodopseudomonas spheroides (upper curve in Fig. 33). From the latter figure we see that its saturation characteristics are not ideally inhomogeneous (see Fig. 7). In Fig. 30 we see that its shape is more nearly Gaussian than Lorentzian (disregarding the slight asymmetry that is observed). When these facts are taken in conjunction with the temperature dependence of the amplitude, and decay time (Fig. 31), it must be concluded that the observed resonance is still an envelope containing several narrower lines arising from quite different electrons.

Recently we have been working with chromatophores from the red photosynthetic bacteria Rhodospirillum rubrum. These are small spherical particles approximately 200 Å in diameter, and containing all of the light absorbing pigments of the whole bacteria. These particles will perform cyclic photophosphorylation reactions.

The sample of chromatophores is suspended in an appropriately buffered aqueous medium (50, 51). Photo induced resonance absorptions are observed. In g-value, width, and shape these signals seem to be the same as observed in the whole bacteria (see Fig. 30). The rise and decay times of the signal are somewhat altered as might be expected when the terminations of the energy transfer system have been removed. In particular, at room temperature the decay scheme contains a fast and a slow component, whereas the whole cell in aqeuous suspension has only a single fast component.

Where the spin concentration is photo induced it is of some interest to determine the action spectrum of the equilibrium spin concentration as a function of the wavelength of the incident light. In previous attempts to obtain such a spectrum (52) the sample has been infinitely thick compared to the distance the active light penetrates into the sample. Self-absorption effects were pronounced, shifting the maximum of the action spectrum to the long wavelength side of the chlorophyll absorption maximum. The chromatophore sample used here was only slightly colored to the eye (the O.D. recorded in Fig. 32 represents a sample of

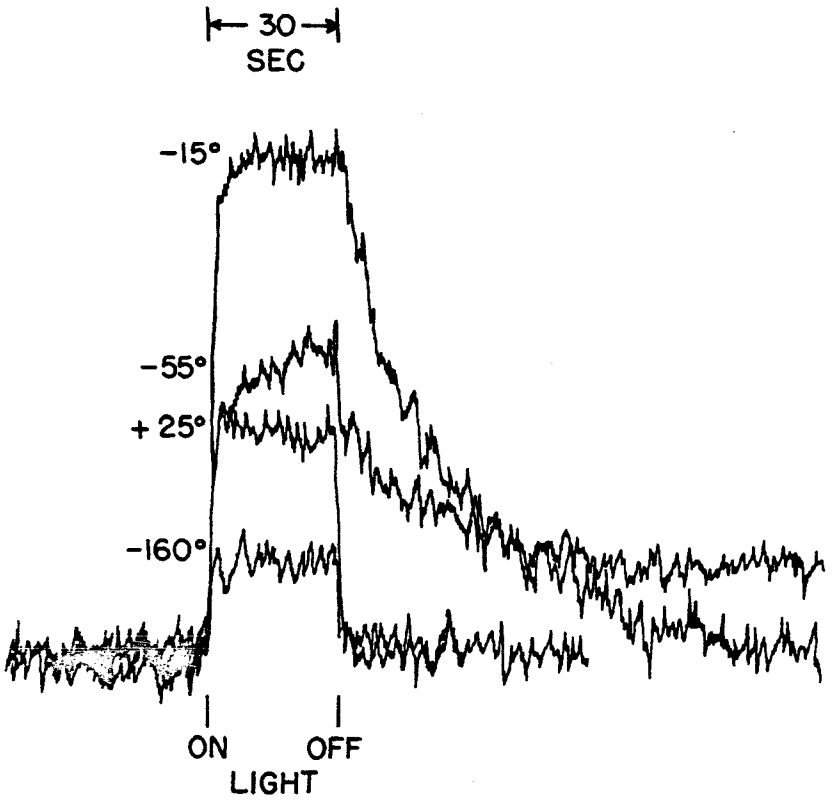

RISE AND DECAY OF ESR SIGNALS
FROM *RHODOSPIRILLUM RUBRUM*

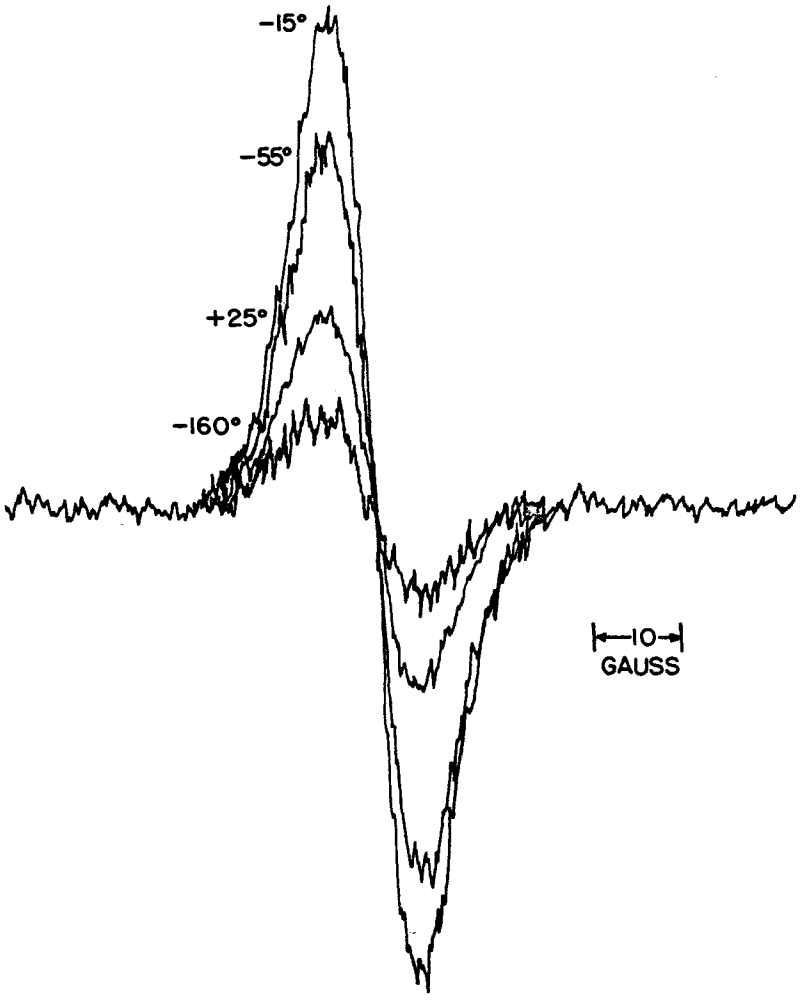

ESR SIGNALS FROM *RHODOSPIRILLUM RUBRUM*
5 MINUTES CONTINUOUS ILLUMINATION

Fig. 31. Shape, amplitude, and rise and decay kinetics of the epr signal in Rhodospirillum rubrum as a function of temperature. Dried film.

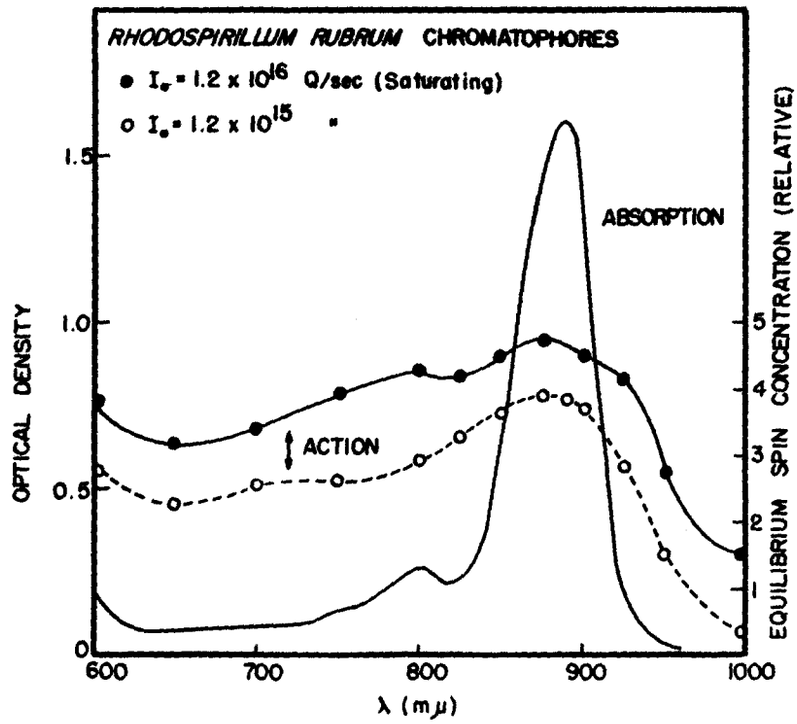

Fig. 32. Action spectrum of Rhodospirillum rubrum chromatophores.

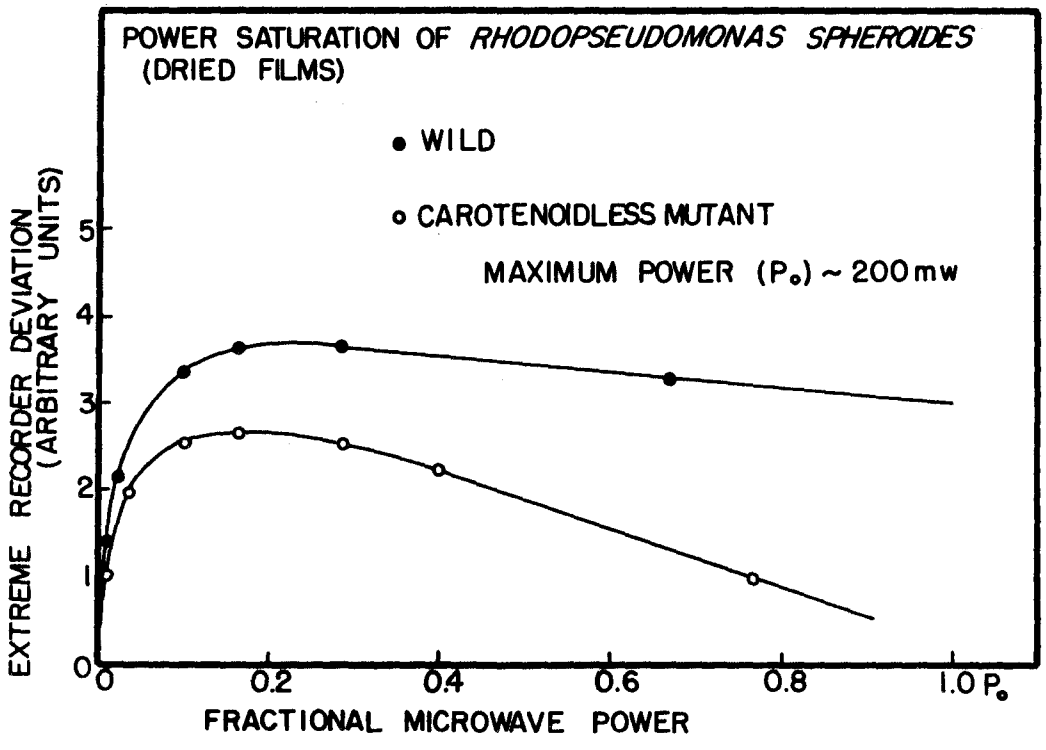

Fig. 33. Power saturation of the epr in the wild and a mutant type of Rhodopseudomonas spheroides. Dried films at room temperature.

the same thickness, but a factor of 3.3 greater in concentration than those used in the spin determination). As is seen in Fig. 32, the action spectrum now peaks at the absorption maximum of the bacterial-chlorophyll. This spectrum probably still suffers somewhat from self-absorption effects, but is nearer the true situation. It is evident that bacterial chlorophyll is the principle pigment responsible for spin production.

No accurate absolute T_1 measurements have as yet been made on radicals appearing in biological systems. In photosynthetic systems they appear to be on the order of 10^{-6} seconds at room temperature. Some relative T_1 measurements have been made. Allen, et al. (48) report that, of the two overlapping photo induced resonances observed in chloroplasts and green algae, the narrow (fast rising and decaying) one saturates more easily.

In our laboratory we have studied the red bacteria Rhodopseudomonas spheroides and a blue green mutant of this bacteria which lacked the carotenoid pigments. (53) One difference in behavior which was noted was the way in which the two resonances saturated. This is shown in Fig. 33. The wild type seems to saturate more like an inhomogeneously broadened system than does the mutant, and to have a somewhat shorter relaxation time. The physical parameters of the two resonances were otherwise the same. This would suggest that the mutant has fewer varieties of unpaired electrons participating in the production of this signal.

Deuteration has been used in one experiment involving photosynthetic systems. Commoner (47) reports epr observations on Chlorella cultured in 99.9% D_2O growth medium by Katz. (54) Both resonances observed in Chlorella were significantly narrowed by the substitution of D for H.

Mutants occasionally supply unique opportunities for insight into the mechanisms of radical formation in photosynthetic systems. Allen et al. (48)

have observed two overlapping resonance lines in several green algae. Some of their results for Chlorella are reproduced in Fig. 34. The dependence of the relative signal amplitude on the wavelength of the light incident on the sample made it probable that the two resonance lines were resulting from the absorption of light by two different pigment systems. The pigment system absorbing the light which was producing the broader resonance was implicated with chlorophyll b by using a Chlorella mutant in which this pigment was absent. In this latter case the broad resonance failed to appear.

In what has been said concerning the formation of unpaired electrons in photosynthetic systems, the question of their role in quantum conversion has not been raised. No one has yet shown that they play any significant role in natural photosynthesis. It has been shown (20) that etiolated leaves fail to show photo induced spins. We have attempted to inquire further into the possible role of the radical in photosynthesis using a yellow (chlorophyll-less) mutant of Chlamydomonas*.

---

* Supplied by Dr. Ruth Sager.

In this experiment 6 flasks of cell cultures were grown anaerobically in the dark until the total cell volume per flask was sufficient for the needs of the experiment. When this condition was fulfilled all 6 flasks were exposed to uniform illumination. At this time the total chlorophyll content of the cells was very low. On being exposed to light, though, the cells start to revert, regaining their total chlorophyll compliment in 15 hours. One flask of cells was harvested immediately after exposure to light. The others were harvested at intervals of 3 hours thereafter. The uniform illumination in which the cell cultures were reverting ($\sim$ 700 foot candles) was approximately 5 to 10 times smaller than the illumination to which they were exposed in the later parts of

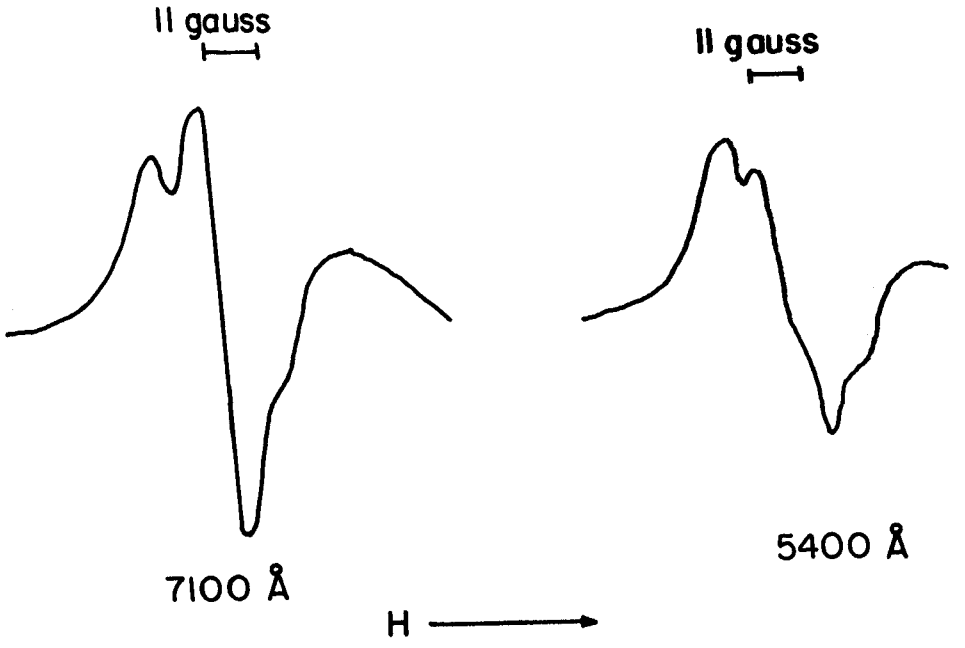

Fig. 34. Light induced epr signals in Chlorella pyrenoidosa at two different wavelengths of illumination. (After 48)

the experiment. The later parts consisted of several independent measurements, as follows. On each cell sample, a chlorophyll content, an O_2 evolution rate, a CO_2 fixation rate, and an equilibrium epr signal amplitude (using white light in each case) were determined. The O_2 evolution and CO_2 fixation experiments were performed on very dilute suspensions so that variation in observed rates can be attributed to physiological changes in the cell, and not to the shielding effects of an optically dense suspension. The epr experiments were performed on very dense aqueous suspensions so that, excepting possibly the first one or two measurements at zero time and at 3 hours, all of the light is absorbed by the sample. All of these measurements were normalized to the same volume of wet packed cells.

Our preliminary results are plotted in Fig. 35. The equilibrium epr amplitude, the rate of $C^{14}O_2$ fixation, and the rate of O_2 evolution are all normalized so that the maximum value observed in each variable is equal to one. These are plotted against chlorophyll (a + b) content, also normalized to one at maximum value. The chlorophyll (a + b) concentration as a function of time is given in Table III.

Table III

Time (hours)	0	3	6	9	12	15
Relative chlorophyll (a + b) concentration	0.05	0.08	0.20	0.80	0.84	1.00*

* Corresponds to 2.7 mg chlorophyll (a + b)/ml wet packed cells.

There are several clear results: 1) An epr signal grows in as the chlorophyll content increases. 2) The relationship between chlorophyll content and epr amplitude is not linear, the larger part of the signal amplitude growing with

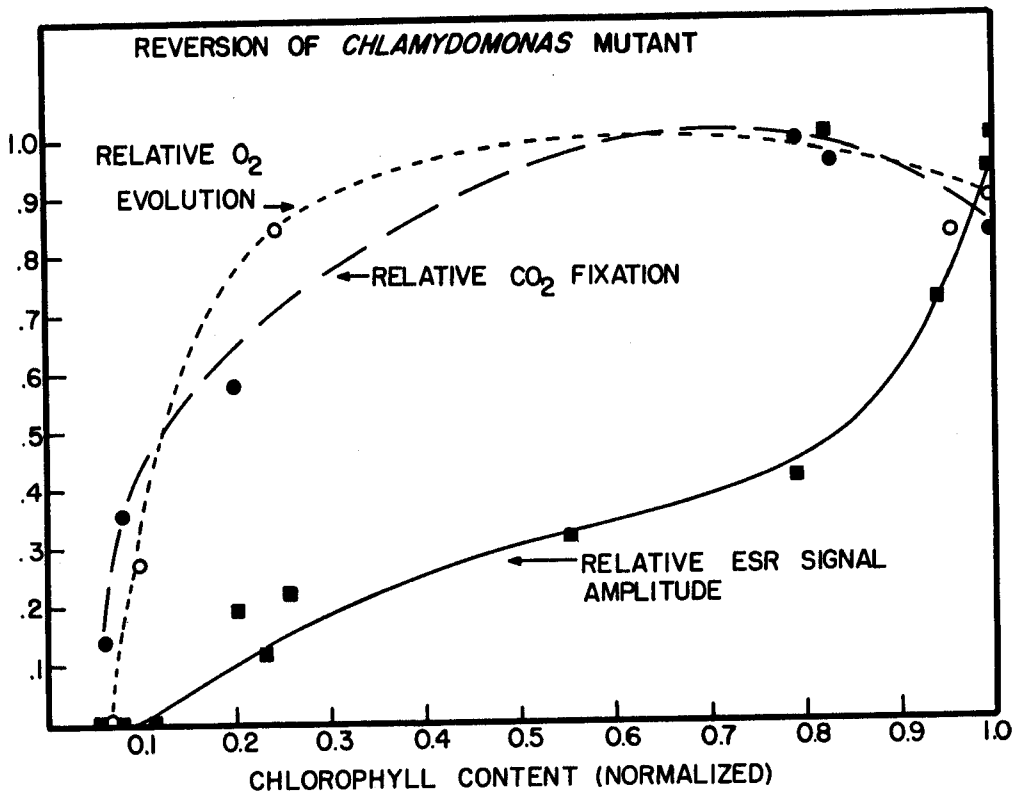

Fig. 35. The epr amplitude, O_2 evolution rate, $C^{14}O_2$ fixation rate as a function of chlorophyll (a + b) content during the reversion to wild type of a yellow mutant of Chlamydomonas reinhardi. The esr amplitude recorded is the composite of two overlapping lines. These lines have been resolved in older cultures, but instrument sensitivity has prevented our resolving them during the reversion peridd. The observed line shape and the concentration ratio of chlorophyll a/chlorophyll b remain constant during the reversion.

the last 20% of the chlorophyll synthesized. 3) The rate of photosynthesis, as measured by the rate of O_2 evolution, and the rate of turnover of the carbon cycle, as measured by the rate of $C^{14}O_2$ fixation, are maximal long before the epr amplitude starts its steepest rise. These suggest that as the concentration of light absorbing pigments passes a certain level, the energy absorbing ability of the pigments is no longer the limiting factor in the over-all reaction; some other process becomes limiting. This may be represented schematically as follows:

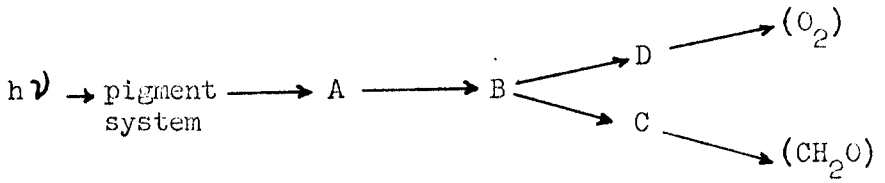

As the energy absorbing ability of the pigment system increases step A ⟶ B (say) becomes limiting. This allows pools of A, etc., and excited pigment molecules to build up. In this view the radicals would then be in any or all of these pools.

The steepest rise of signal amplitude as the last chlorophyll is synthesized suggests also that the highest efficiency for spin production is dependent upon the completion of some structural element containing chlorophyll.

Some of these unpaired electrons are formed in the light and disappear in the dark at rates which are only very slightly, if at all, dependent on the temperature (Fig. 31). (55) We would suggest that these are the electrons resulting from the initial quantum conversion act. The unpairing and separation of a pair of electrons into two separate sites in a process which is nearly temperature independent constitutes the initial conversion into physical and chemical potential energy. One of these unpaired electrons would reside in the pigment system itself (chlorophylls), the other would be associated with one or another of the several concomitant molecules (cytochrome, manganese, porphyrin, quinone, disulfide, flavin) in the photosynthetic apparatus. The other pertinent evidence

for this basic idea has been reviewed elsewhere (56) and includes direct observation of such photo induced electron transfer from cytochrome as well as photo induced electron transfer in donor-acceptor model systems (57).

REFERENCES

1. H. White, Introduction to Atomic Spectra, p. 215, McGraw Hill, New York (1934).
2. E. Zavoisky, J. Phys. U.S.S.R., 9, 211 (1945).
3. R.L. Cummerow and D. Halliday, Phys. Rev., 70, 433 (1946).
4. W. Köhnlein and A. Müller, Free Radicals in Biological Systems, p. 113, Academic Press, New York (1961).
5. V. Wertz and J. Vivo, J. Chem. Phys., 23, 2441 (1955).
6. E.M. Roberts and W.S. Koski, J. Amer. Chem. Soc., 82, 3006 (1960).
7. J. Eastman, unpublished results.
8. B.G. Malmstrom and T. Vanngard, J. Mol. Biol., 2, 118 (1960).
9. M.S. Blois, H.W. Brown, and J.E. Maling, Free Radicals in Biological Systems, p. 117, Academic Press, New York (1961).
10. D.J.E. Ingram and J.E. Bennett, Discussions Faraday Soc., 19, 140 (1955).
11. J.E. Bennett, J.F. Gibson, and D.J.E. Ingram, Proc. Roy. Soc. (L), A 240, 67 (1957).
12. J.F. Gibson and D.J.E. Ingram, Nature, 180, 29 (1957).
13. A.M. Portis, Phys. Rev., 91, 1071 (1953).
14. O.S. Liefson and C.D. Jeffries, Phys. Rev., 122, 1781 (1961).
15. G. Feher, Phys. Rev., 114, 1219 (1959).
16. G. Feher, Proceeding Kamerlingh Onnes Conference on Low Temperature Physics, Leiden, June 1958, p. 83, Supplement to Physica, Sept. 1958.
17. C.A. Hutchinson and B.W. Mangum, J. Chem. Phys., 29, 952 (1958).
18. T.H. van der Waals and M.S. de Groot, Mol. Phys., 2, 333 (1959).
19. T.H. van der Waals and M.S. de Groot, Mol. Phys., 3, 190 (1960).
20. B. Commoner, J. Townsend, and G.E. Pake, Nature, 174, 689 (1954).
21. B. Commoner, J.J. Heise and J. Townsend, Proc. Nat. Acad. Sci., 42, 710 (1956).
22. P.B. Sogo, N.G. Pon and M. Calvin, Proc. Nat. Acad. Sci. U.S., 43, 387 (1957).

23. R.H. Sands, NMR and EPR Spectroscopy, p. 233, Pergamon Press, New York (1960).

24. M.S. Blois and J.E. Maling, Biochem. Biophys. Res. Comm., 3, 132 (1960).

25. R.O. Lindblom, R.M. Lemmon and M. Calvin, J. Amer. Chem. Soc., 83, 2484 (1961).

26. J.E. Wertz, D.C. Reitz, F. Draunieks, Free Radicals in Biological Systems, p. 183, Academic Press, New York (1961).

27. L.A. Bliumenfel'd, Biofizika, 4, 515 (1959).

28. L.A. Bliumenfel'd and V.A. Benderskii, Dokl. Acad. Nauk. U.S.S.R., 133, 1451 (1960).

29. L.A. Bliumenfel'd, A.F. Kalmanson, and Sheng Pei-ken, Dokl. Acad. Nauk. U.S.S.R., 124, 1144 (1959).

30. M.S. Blois and J.E. Maling, Biochem. Biophys. Res. Comm. (in press).

31. M.S. Blois and J.E. Maling, Biochem. Biophys. Res. Comm., 4, 252 (1961).

32. I. Isenberg, Biochem. Biophys. Res. Comm., 5, 139 (1961).

33. H. Shields and W. Gordy, Proc. Nat. Acad. Sci. U.S., 45, 269 (1959).

34. D. Libby, M.G. Ormerod, and A. Charlesby, Nature, 190, 998 (1961).

35. I. Miyagawa and W. Gordy, Rad. Res., 12, 211 (1960).

36. V. Holmogorov and A. Terenin, Naturwissenschaften, 48, 158 (1961).

37. A.F.H. Anderson, unpublished results.

38. A.A. Krasnovskii, N.N. Bubnov, A.V. Umrikhina, V.F. Tsepalov and V. Ia. Shliapintokh, Biofizika, 5, 121 (1960).

39. I. Yamazaki, H.S. Mason and L. Piette, J. Biol. Chem., 235, 2444 (1960).

40. T.E. King, R.L. Howard and H.S. Mason (to be published).

41. H. Beinert and R.H. Sands, Biochem. Biophys. Res. Comm., 3, 41 (1960).

42. H. Beinert and R.H. Sands, Biochem. Biophys. Res. Comm., 3, 47 (1960).

43. H. Beinert and W. Lee, Biochem. Biophys. Res. Comm., 5, 40 (1961).

44. T. Vänngard, R.C. Bray, B.G. Mälmstrom and R. Pettersson, Free Radicals in Biological Systems, p. 209, Academic Press, New York (1961).

45. W. Gordy, W.B. Ard and H. Shields, Proc. Nat. Acad. Sci., 41, 983 (1955).

46. T. Henriksen, Free Radicals in Biological Systems, p. 279, Academic Press, New York (1961).

47. B. Commoner, Light and Life, p. 356, Johns Hopkins Press, Baltimore (1961).

48. M.B. Allen, L.H. Piette, and J.C. Murchio, Biochem. Biophys. Res. Comm., 4, 271 (1961).

49. H.E. Weaver, private communication.

50. A.W. Frenkel and D.D. Hickman, J. Biophys. Biochem. Cytology, 6, 285 (1959).

51. For the cell used to insert water into the cavity see, for example, L. Piette, I. Yamazaki and H.S. Mason, Free Radicals in Biological Systems, p. 195, Academic Press, New York (1961).

52. P.B. Sogo, L.A. Carter, M. Calvin, Free Radicals in Biological Systems, p. 311, Academic Press, New York (1961).

53. M. Griffiths, W. Sistrom, G. Cohen-Bazire, and R.Y. Stanier, Nature, 176, 1211 (1955).

54. W. Chorney, N.J. Scully, H.L. Crespi and J.J. Katz, Biochem. Biophys. Acta, 37, 280 (1960).

55. P.B. Sogo, M. Jost and M. Calvin, Rad. Res. Suppl., 1, 511 (1959).

56. M. Calvin, J. Theor. Biol., 1, 258 (1961); M. Calvin (to be published in Perspectives in Biology and Medicine.)

57. D. Kearns and M. Calvin, J. Amer. Chem. Soc., 83, 2110 (1961).; J. Eastman, G. Androes, and M. Calvin (to be published in J. Chem. Phys.).